UNIVERSITY OF CALIFORNIA
SANTA CRUZ

OVERLAPPING AND DISTINCT ROLES OF TWO *C. ELEGANS* H3 LYSINE 36 HISTONE METHYLTRANSFERASES

A dissertation submitted in partial satisfaction
of the requirements for the degree of

DOCTOR OF PHILOSOPHY

In

MOLECULAR, CELL, AND
DEVELOPMENTAL BIOLOGY

By

Jeremy Kreher

September 2017

The Dissertation of Jeremy Kreher is approved:

_____
Professor Susan Strome, Chair

_____
Professor John Tamkun

_____
Professor Grant Hartzog

_____
Tyrus Miller
Vice Provost and Dean of Graduate Studies

TABLE OF CONTENTS

LIST OF FIGURES

ABSTRACT

Overlapping and Distinct Roles of Two *C. Elegans*

H3 Lysine 36 Histone Methyltransferases

Jeremy Kreher

Establishment and maintenance of cell type-specific gene expression patterns is essential for development and normal tissue function. A growing number of studies demonstrate that epigenetic information contributes to cell fate specification and maintenance, and can be transmitted though mitotic divisions as well as from parents to progeny. Yet, the mechanisms involved in establishing and maintaining epigenetic information, as well as the consequences to gene expression in cells inheriting epigenetic information are not well understood. One form of epigenetic information, post-translational modifications of histones, can regulate gene expression patterns and provide a long-term memory of expression patterns established by transient transcription factor activity during early development. In *C. elegans,* two antagonistic histone methyltransferases (HMTs) are essential for germline development in a maternal effect manner. MES-2 is part of a PRC2-like complex that methylates H3 lysine 27 (H3K27me3), and MES-4 is one of two H3K36me3 HMTs. This thesis focuses on H3K36me3 and the two enzymes that generate this mark, MES-4 and MET-1. While MES-4 is required for germline development in all conditions, MET-1 is only required at elevated temperatures. Our mass spectrometry analysis of histone tails from *C. elegans* early embryos confirmed that both MET-1 and MES-4 catalyze H3K36me3, a modification that is generated by only a single enzyme in other organisms. We performed immunostaining studies to investigate the generation of H3K36me3 in the adult germline, its transmission from parents to progeny, and its maintenance during early embryogenesis. Our data show that MET-1 and MES-4 serve unique roles in the generation and transmission of H3K36me3. In the germline, MET-1 co-transcriptionally catalyzes H3K36me3 and is solely responsible for H3K36me3 on the oocyte

X chromosome. MES-4 also contributes to H3K36me3 in the germline and is solely responsible for maintenance of H3K36me3 on chromosomes in early embryos, where it operates in a transcription-independent manner.

We discovered that both oocytes and sperm transmit chromosomes carrying H3K36me3 to the embryo. This observation supports the hypothesis that epigenetic information generated in the adult germline can be transmitted to progeny from either parent. To determine if inherited H3K36me3 is required for MES-4 to associate with chromosomes, we generated embryos in which only a subset of chromosomes carry H3K36me3. In these embryos, MES-4 is recruited to H3K36me3-positive chromosomes but not to H3K36me3-negative chromosomes, suggesting MES-4 is recruited to chromosomes by pre-existing H3K36me3. Additionally, as these embryos divide, MES-4 and H3K36me3 are maintained on only a subset of chromosomes until at least the 32-cell stage, likely because MES-4 is propagating H3K36me3 in regions of chromatin with pre-existing H3K36me3. This observation suggests that MES-4 maintains an epigenetic memory of inherited H3K36me3. Together, these data support the model that MET-1 is primarily responsible for generating H3K36me3 on genes expressed in the germline, and that MES-4 is primarily responsible for maintaining an epigenetic memory of inherited H3K36me3 through early embryogenesis, likely to guide gene expression patterns in nascent germ cells.

ACKNOWLEDGMENTS

I'd like to extend my appreciation to:

Susan Strome for the opportunity to train in your lab. Thank you for your mentorship, scientific and otherwise. I admire your scientific creativity, clarity, and enthusiasm to work outside your expertise if required. In addition to your strengths as a scientist, I also admire your remarkable ability to be both professional and compassionate. I'll do well if I take with me only a fraction of your aptitude for science and thoughtfulness and tact you employ when working with others.

John Tamkun, Grant Hartzog, and Needhi Bhalla for serving as both my qualifying exam and thesis committee. Thank you for your time and your insight. I feel fortunate for having such a strong committee and truly would have enjoyed more meetings and discussion than we had. I deeply value your expertise, critiques, and advice.

My friends and family for their support prior to and during my graduate work. Thank you for the encouragement you have given me along the way and for being there through thick and thin. I know I can always count on you, and I aspire to do the same for you.

My fellow Stromies, past and present. The level of enthusiasm, dedication, and knowledge you brought to the lab was enriching. Thank you for the discussions, guidance, and friendship. My time in the lab with you was a wonderful experience.

Alesa Byers for reminding me to stop and smell the roses, as they say. Your appreciation for life is extremely infectious and your desire to make the best of it for yourself and others should be equally transmissible. Thank you for so many interesting and perception-changing conversations, I'm grateful for having you in my life.

CHAPTER 1: INTRODUCTION

Differential gene expression gives rise to unique cell types.

All differentiated cells in mature multicellular organisms have a nearly identical genome. Yet, these organisms are comprised of cells that exhibit a variety of shapes, sizes, and functions. The diversity of cell types is achieved by differential gene expression. As cells divide during development, their gene expression patterns may begin to diverge from their parent or sister cell. In this way, each cell type ultimately expresses a unique set of genes and therefore a unique complement of RNAs and proteins. Fundamentally, cell identity is determined by a cell's complement of RNAs and proteins.

Gene expression is regulated by chromatin organization.

Cells are capable of regulating gene expression at many levels, including transcription, RNA processing, translation, and post-translational modification of proteins. Regulation at each of these steps contributes to establishing and maintaining cell identity. Transcriptional regulation can be achieved by altering DNA accessibility to the transcriptional machinery. Gene expression depends on the ability of transcription factors to recognize and bind DNA sequences, so it follows that rendering regulatory DNA sequences more or less accessible can impact expression of the associated gene.

In eukaryotic nuclei, DNA is packaged into chromatin, which is organized into varying levels of compaction (Figure 1-1). The first level of packing entails the wrapping of ~147 bp of DNA around an octamer of histones to form the most basic unit of chromatin, the nucleosome (Olins and Olins 1974; Kornberg 1974). Additional levels of compaction, or higher order chromatin structures, can be achieved by a yet-to-be-determined manner of coiling. Each nucleosome consists of two histone H2A and H2B dimers and a histone H3 and H4 tetramer (Olins and Olins 1974; Kornberg 1974; Luger and Richmond 1998); post-translational modification of these histones can influence chromatin compaction (Figure 1-2) (Bannister

and Kouzarides 2011). Chromatin organization is dynamic but can be classified into two general states, heterochromatin and euchromatin. Heterochromatin is usually highly condensed and associated with repressed regions of the genome, whereas euchromatin is more loosely packed and associated with active regions of the genome (Jenuwein and Allis 2001; Grewal and Elgin 2002). Regulation of chromatin is mainly achieved by nucleosome remodelers, incorporation of histone variants, and post-translational modification of the histone core and N-terminal tails. The effect of post-translational modification of histones on chromatin organization depends on which histone residues are modified and what combination of modifications are present within a nucleosome or region of chromatin (Strahl and Allis 2000). The growing list of known histone modifications includes, but is not limited to, ubiquitination, phosphorylation, acetylation, and methylation (Figure 1-2) (Bannister and Kouzarides 2011). Focusing on methylation, repressed chromatin is enriched for methylation of histone H3 at lysine 27 (H3K27me) and H3K9me, whereas active chromatin is enriched for H3K4me and H3K36me (Jenuwein and Allis 2001) (Gerstein *et al.* 2010) Seminal experiments in *Drosophila* demonstrated the ability of heterochromatin to spread along the chromosome and silence genes that become packaged into heterochromatin (Muller 1930; Ebert *et al.* 2006). There is an ongoing debate over whether transcriptional activity is a cause or consequence of chromatin states, but the most likely explanation is that it is both, and context dependent.

A memory of gene expression patterns can be encoded in histone modifications and can be transmitted through cell divisions.

One of the best-understood examples of chromatin-based regulation is *HOX* gene regulation during *Drosophila* development (Kassis *et al.* 2017). During embryogenesis, a group of transcription factors, encoded by the segmentation genes, establishes a pattern of active and repressed transcription states of developmental genes, including the homeotic or *HOX* genes (Figure 1-3). Although the expression and activity of these transcription factors are transient,

HOX gene expression patterns are maintained through development. Maintenance of the repressed state requires the activity of the conserved Polycomb Repressive Complex 2 (PRC2), which generates the repressive mark H3K27me3. Once established, the current model is that the silent state is self-reinforced, in part, by binding of PRC2 to H3K27me3-marked chromatin and propagating the same mark on nearby nucleosomes (Figure 1-3) (van Kruijsbergen *et al.* 2015). Long-term maintenance and propagation of chromatin states must be maintained in the face of nucleosome disruption that occurs during DNA replication and transcription. Both of these processes must disassemble nucleosomes to access the DNA strand. Therefore, histone modifications present before disassembly of the nucleosome could be lost during reassembly of nucleosomes behind either polymerase complex. Reestablishment of the original chromatin state could occur through reincorporation of histones from the parental chromatin fiber and/or by local concentrations of histone methyltransferases (HMTs) that modify newly incorporated histones. There is evidence for both. Studies of *Drosophila* S2 cells and *C. elegans* embryos suggest H3K27me3 marked histones are redeposited behind the DNA replication fork {Lanzuolo:2011fz, Gaydos:2014ci}. Conversely, Petruk et al. reported Trx, Pc, and E(z) are associated with nascent DNA following replication, but H3K4me3 and H3K27me3 marked histones are not redeposited {Petruk:2012iz}. These conflicting results could be a consequence of using different assays or analysis of different organisms and/or developmental stages.

The consequences of H3K36 methylation are variable and depend on the organism, chromatin context, and genomic position.

In contrast to the Polycomb Group (PcG) of proteins, which maintains the memory of repression in *Drosophila*, the Trithorax Group (TrxG) of proteins maintains the memory of active gene expression that was established during embryogenesis (Kassis *et al.* 2017). The TrxG includes the H3K36 HMT ASH1, which deposits H3K36me2 on active genes and antagonizes the activity of PRC2 at those genes (Tanaka *et al.* 2007; Yuan *et al.* 2011;

Dorighi and Tamkun 2013). Antagonism of H3K27me3 by H3K36me2 and me3 is conserved and has been demonstrated in multiple organisms using *in vivo* and *in vitro* assays (Tanaka *et al.* 2007; Yuan *et al.* 2011; Schmitges *et al.* 2011; Gaydos *et al.* 2012; Dorighi and Tamkun 2013). Whereas H3K27me3 is considered to be a repressive mark in most contexts, the consequences to gene expression of marking of chromatin with H3K36me varies depending on the organism and the local chromatin context. H3K36me is generally associated with actively transcribed genes, is distributed across the gene body, and has been shown to play a role in regulating gene expression, DNA replication and repair, alternative splicing, and nucleosome exchange (Wagner and Carpenter 2012; McDaniel and Strahl 2017).

Eukaryotic H3K36-specific HMTs are well conserved SET domain-containing proteins. Many H3K36 HMTs also contain a PWWP domain that can bind H3K36me2 (Sankaran *et al.* 2016) or H3K36me3 (Wu *et al.* 2011; Wagner and Carpenter 2012; Qin and Min 2014). The yeast *Saccharomyces cerevisiae* possesses only a single H3K36 HMT, Set2, which performs mono-, di-, and tri-methylation of H3K36. Set2 methylates actively expressed genes co-transcriptionally through association with elongating RNA Polymerase II (RNAPII) (Li *et al.* 2002). The Set2 Rpb1 Interacting (SRI) domain of Set2 facilitates interaction between Set2 and elongating RNAPII by binding to the hyperphosphorylated carboxyl-terminal domain (CTD) of RNAPII (Kizer *et al.* 2005) (Figure 1-4). This interaction focuses Set2's HMT activity on the body of genes, where H3K36me is usually detected in yeast and many other organisms (Strahl *et al.* 2002; Xiao *et al.* 2003; Krogan *et al.* 2003; Rao *et al.* 2005; Barski *et al.* 2007; Bell *et al.* 2007; Furuhashi *et al.* 2010; Rechtsteiner *et al.* 2010). Although H3K36me in yeast is found on active genes, it serves a repressive role. Expressed genes acquire co-transcriptional histone acetylation, which leaves chromatin in a less compact state and more permissive to transcription from cryptic promoters within the gene body (Figure 1-4). Ectopic transcripts from internal cryptic promoters are detected in *Set2* mutants. The role of H3K36me on active yeast genes is to stabilize and stimulate the activity of the Rpd3 small

(Rpd3s) histone deacetylase complex (HDAC), which resets chromatin to a repressive state and prevents transcription factors from accessing cryptic promoters (McDaniel and Strahl 2017).

Unlike yeast, most other eukaryotes possess multiple H3K36 HMTs. And with the exception of *C. elegans*, the HMTs appear to be specific for either H3K36me1/2 or H3K36me3 (Wagner and Carpenter 2012). Different levels of H3K36 methylation in *Drosophila* lead to different gene expression outcomes. *NSD* encodes a H3K36me2-specific HMT, and Set2, an essential gene, encodes an H3K36me3 HMT. Like most H3K36me3 HMTs, *Drosophila* Set2 associates with RNAPII and co-transcriptionally methylates histones in the body of active genes (Stabell *et al.* 2007; Bell *et al.* 2007). In *Drosophila* Kc cells, reduced NSD-dependent H3K36me2 leads to global hypoacetylation, whereas reduced Set2-dependent H3K36me3 leads to global hyperacetylation (Bell *et al.* 2008). In males, reduced H3K36me3 leads to hyperacetylation on the autosomes, and hypoacetylation on and reduced gene expression from the single X chromosome (Bell *et al.* 2008). In this context, the function H3K36me3 is to stabilize binding of the MSL (male sex lethal) histone acetyltransferase (HAT) complex to expressed genes, as part of a mechanism to decondense chromatin and up-regulate expression of X-linked genes in XY males to match autosomal gene expression levels and X-linked gene expression in XX female flies.

The *C. elegans* genome encodes two characterized H3K36me3 HMTs. MET-1 generates H3K36me3 in a co-transcriptional manner, and MES-4 generates H3K36me2 and H3K36me3 (Bender *et al.* 2006; Furuhashi *et al.* 2010; Rechtsteiner *et al.* 2010). MES-4 is unique among H3K36me HMTs in that it can catalyze both di- and tri-methylation of H3K36 (see Chapter 2) and can do so in an RNAPII-independent manner. MES-4 is named for its maternal-effect sterile phenotype, meaning homozygous *mes-4* mutants that receive a maternal load of MES-4 develop into fertile adults while homozygous *mes-4* mutants that do not receive maternal

MES-4 develop into sterile adults (Figure 1-5) (Capowski *et al.* 1991; Garvin *et al.* 1998; Bender *et al.* 2006). Sterile *mes-4* mutants produce the primordial germ cells (PGCs) that would normally proliferate and give rise to the adult germline, but in *mes-4* mutant larvae the germ cells die after minimal proliferation(Capowski *et al.* 1991). The genomic distribution of MES-4, H3K36me3, and RNAPII in early embryos is highly correlated and found within gene bodies, which is consistent with the conventional view that H3K36me3 functions co-transcriptionally. However, MES-4 also maintains H3K36me3 on a small subset of genes that lack RNAPII in embryos. In the absence of MES-4, these genes are not marked by H3K36me3, indicating that MES-4 can function independently of elongating RNAPII (Furuhashi *et al.* 2010; Rechtsteiner *et al.* 2010). Comparison of all MES-4 bound genes in the embryo to genes expressed in adult germlines revealed a significant overlap, suggesting that germline expression, not embryo expression, establishes patterns of H3K36me3 and MES-4 binding in embryos. How MES-4 maintains H3K36me3 through cell divisions in the early embryo is unknown. During DNA replication, pre-existing H3K36me3 will be diluted as parental histones are distributed between the two new DNA strands, and so MES-4 must be recruited to reestablish H3K36me3 levels on the appropriate genes following DNA replication. The current hypothesis is that, in early embryos, MES-4 maintains a memory of genes that were expressed in the parental germline by binding (directly or indirectly) to pre-existing H3K36me3 and propagating the same mark (Figure 1-6). Like the antagonism between TrxG and PRC2 in *Drosophila,* MES-4 and H3K36me3 in *C. elegans* early embryos antagonize H3K27me3. In the absence of MES-4, germline genes lose H3K36me3 and acquire H3K27me3 catalyzed by the *C. elegans* PRC2 complex (MES-2, MES-3, MES-6) (Gaydos *et al.* 2012). These data from worm embryos are reminiscent of the epigenetic memory of *HOX* gene states in *Drosophila* embryogenesis, but with the added importance of a transgenerational (parent to progeny) component. In worm embryos, MES-4 protects germline genes from acquiring repressive H3K27me3 and may deliver a memory of germline-expressed genes to guide the germline gene expression program in PGCs.

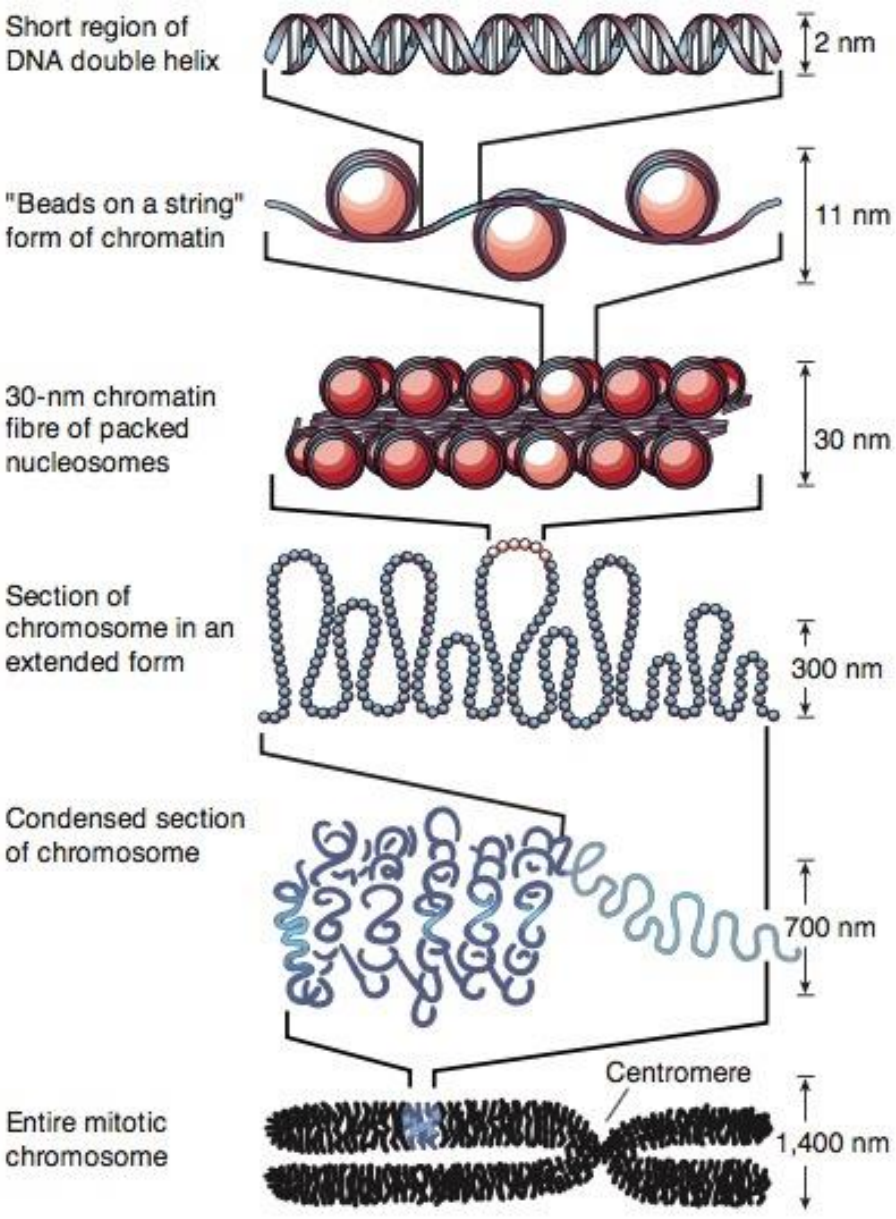

Figure 1-1 The chromatin fiber can be organized into varying levels of compaction. The basic unit of chromatin, the nucleosome, is ~147 bps of DNA wrapped around a histone octamer core. The histone-DNA interactions in the nucleosome can impede interactions between DNA and DNA-binding components of the transcriptional machinery, which can reduce or inhibit gene expression. Beyond the most basic level of compaction, the “beads on a string” organization, additional condensation of the chromatin fiber can further reduce the accessibility of DNA to DNA-binding proteins.

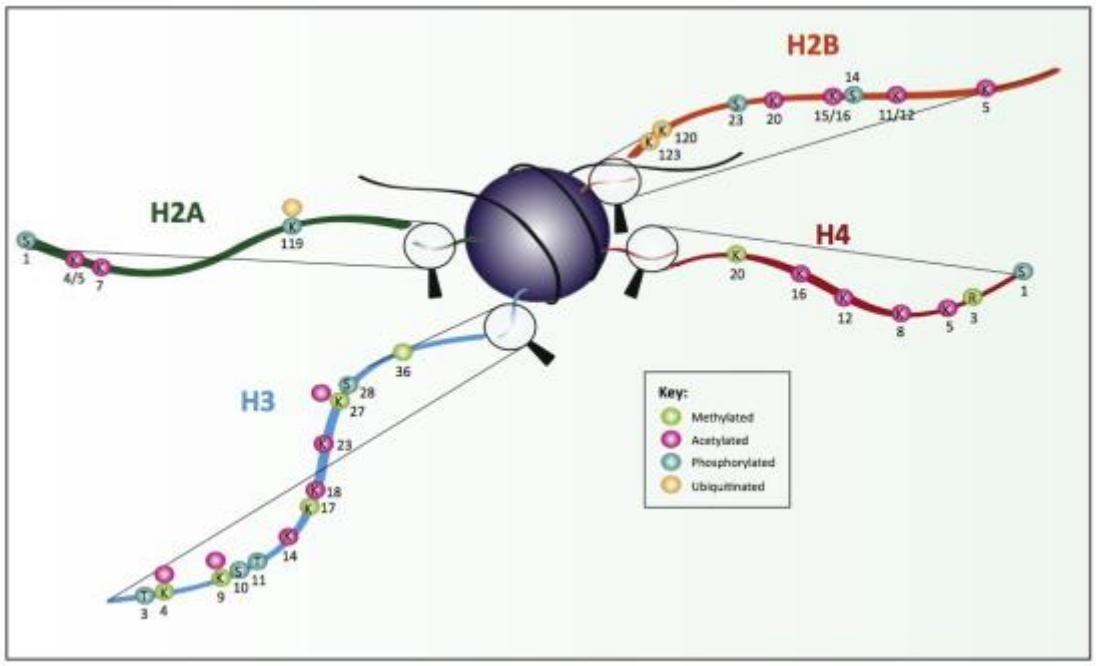

Figure 1-2 Post-translational modifications of nucleosomal histones. Canonical nucleosomes contain a pair of H2A/H2B dimers and an H3/H4 tetramer. Deposition of covalent modifications on the core globular domains or unstructured histone tails can influence the degree to which the chromatin fiber is condensed. Modifications such as acetylation can directly regulate DNA-histone interactions by neutralizing the positive charge on H4 lysine residues, therefore reducing the electrostatic interaction between negatively charged DNA and positively charged lysines. Other modifications, like trimethylation of lysine 36 on H3, can recruit effector proteins that indirectly regulate chromatin structure by removing acetylation, repositioning nucleosomes, or depositing or removing nucleosomes.

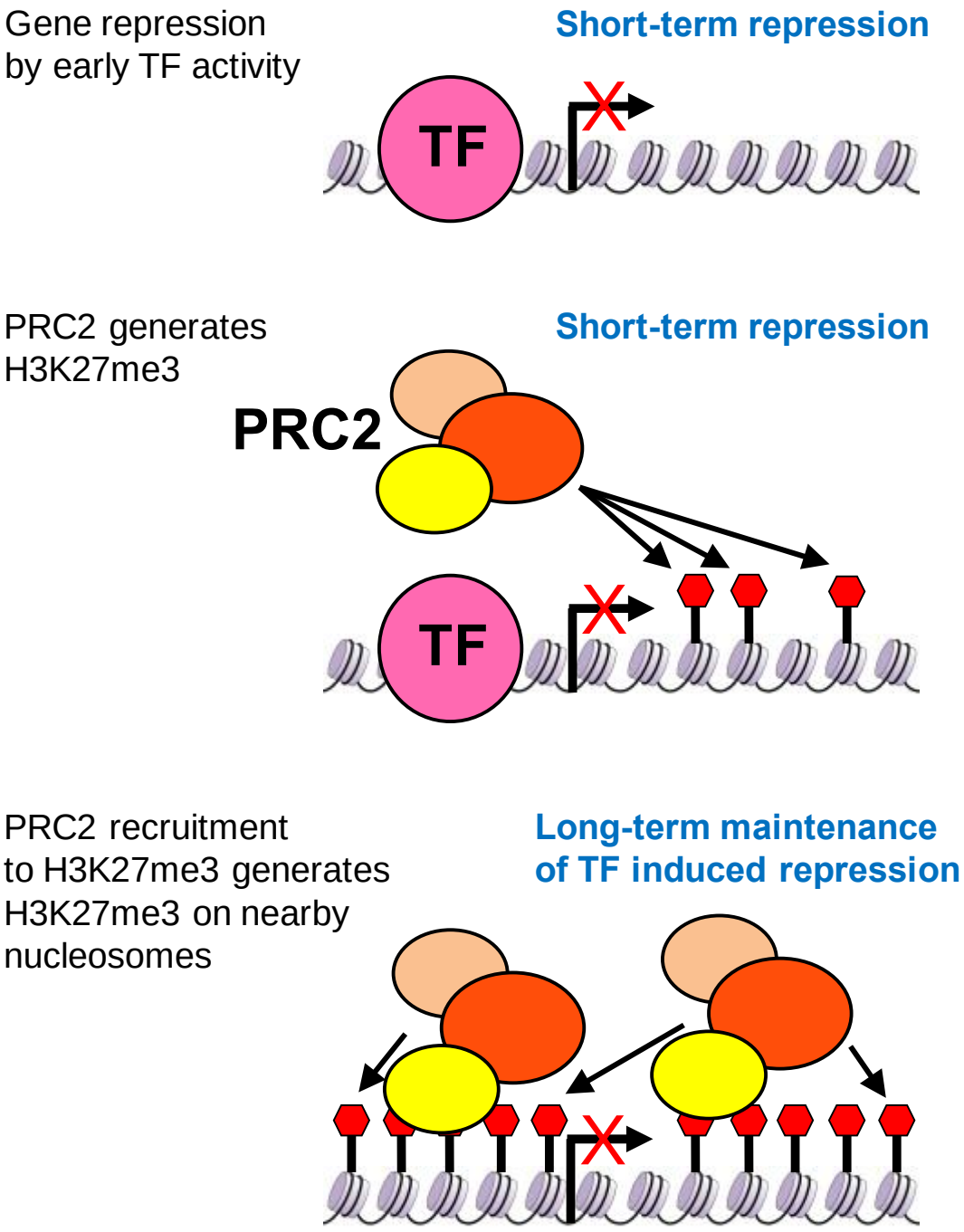

Figure 1-3 Chromatin-based memory of gene silencing. During early Drosophila embryogenesis, sequence-specific transcription factors (TFs) target genes for expression or repression. The repressed state of genes is maintained by chromatin factors, including Polycomb Repressive Complex 2 (PRC2), even after the DBFs are no longer present. This is achieved by tri-methylation of H3K27 by PRC2, and subsequent binding of PRC2 to H3K27me to propagate the modification on nearby nucleosomes through development.

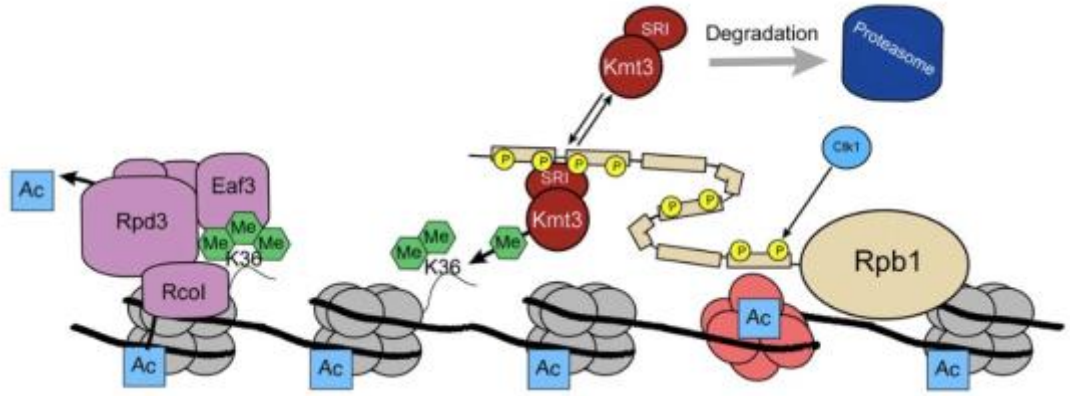

Figure 1-4 Co-transcriptional methylation of H3K36 by Set2. In *Saccharomyces cerevisiae*, Set2 (Kmt3) contains an SRI domain that binds the hyperphosphorylated C-terminal repeats of RNA Polymerase II (Rpb1) during elongation. Set2 co-transcriptionally catalyzes H3K36me within gene bodies, which recruits the Rpd3-containing histone deacetylase complex to remove co-transcriptional acetylation. Deacetylation promotes a more condensed chromatin state that suppresses cryptic initiation from start sites within the gene body.

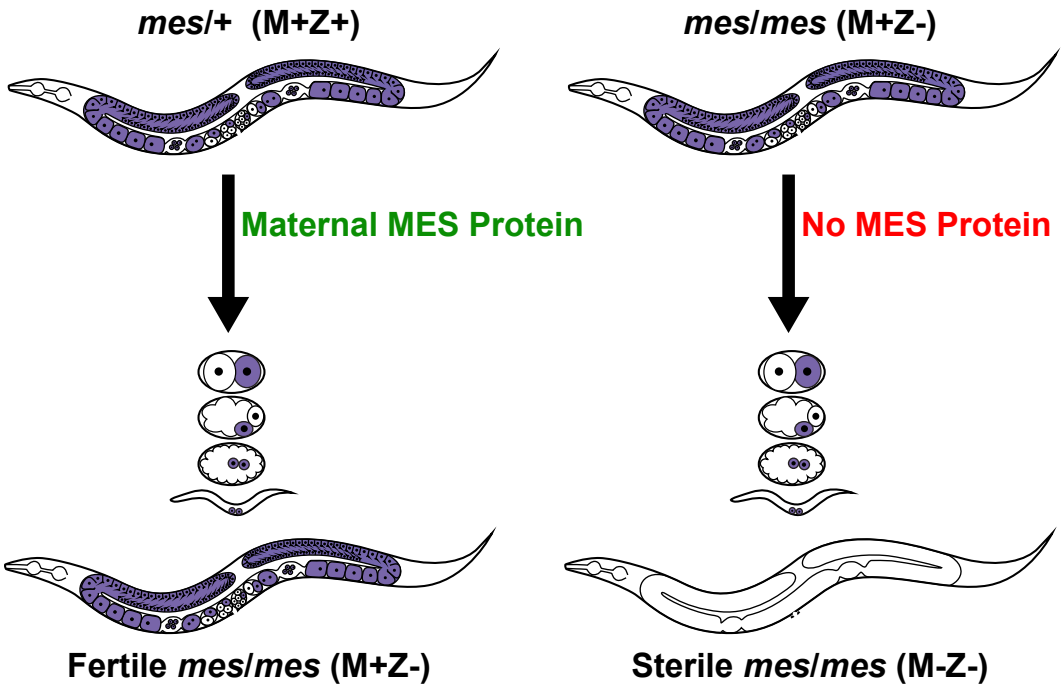

Figure 1-5 The Maternal Effect Sterile (MES) phenotype in *C. elegans*. Homozygous *mes* mutants (M+Z-) from heterozygous mothers are fertile because they receive maternal MES protein. However, homozygous *mes* mutants (M-Z-) from homozygous *mes* mothers are sterile because they do not receive maternal MES protein. Thus, the sterility of *mes* mutants is maternal effect. The first generation of homozygous *mes* mutants are fertile, but the second generation of homozygous *mes* mutants are sterile. (M) Maternal supply of gene product. (Z) Zygotic synthesis of gene product.

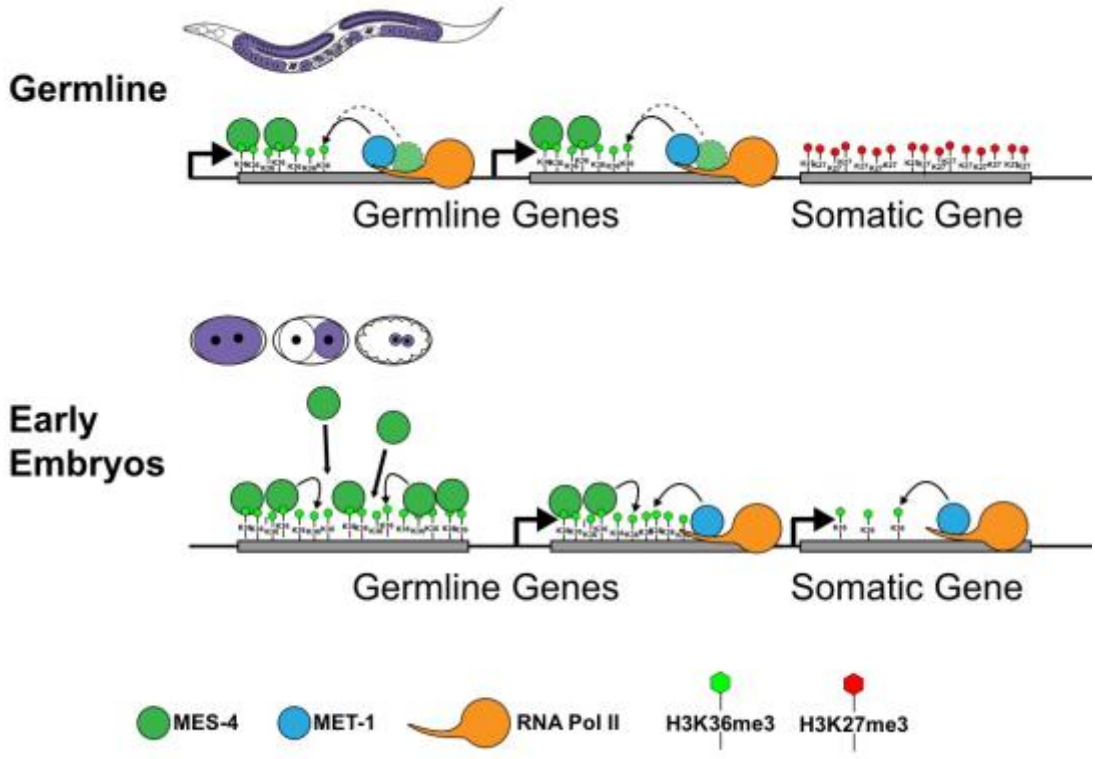

Figure 1-6 Model of MES-4 mediated memory of active gene expression in *C. elegans.* In the parental germline, co-transcriptional MET-1, and perhaps MES-4, activity marks active genes with H3K36me3. Genes that are not expressed in the germline are marked by repressive H3K27me3. Embryos inherit a memory of germline-expressed genes in the form of H3K36me3-marked chromatin. In early embryos, MES-4 maintains pre-existing H3K36me3 patterns independent of RNA Polymerase II activity.

CHAPTER 2: OVERLAPPING AND DISTINCT ROLES FOR TWO *C. ELEGANS* H3 LYSINE 36 HISTONE METHYLTRANSFERASES

Author Contributions

-The work presented in this chapter was inspired by data generated in the Strome lab by Teruaki Takasaki, Andreas Rechtsteiner, and Thea Egelhofer.

-Simone Sidoli, while in the labs of Ole Jensen and Ben Garcia, performed the fragmentation, mass spectrometry analysis of modified histone tails presented in Figure 2-1, and composed the methods for these procedures.

-Linnea Ransom performed the initial experiments for which data is presented in Figure 2-2.

-Teruaki Takasaki acquired the images presented in Figure 2-3B and other preliminary data and images not presented in the figures of this chapter.

-Anthony Rodriguez created the *jhdm-1; jmjd-2; mes-4* strain used for experiments for which data is presenting in figure 2-4.

INTRODUCTION

Multicellular organisms must generate a wide array of cell types from a single cell, the zygote, and must ensure that cell fates are maintained during the lifetime of the organism. Failure to do either can lead to lethality, developmental defects, and cancer. Establishment and maintenance of different cell fates relies on a variety of mechanisms to generate different gene expression patterns between cells that possess an identical genome sequence. One mechanism is packaging sets of genes into chromatin states that are more or less accessible to the transcriptional machinery. The first level of DNA packaging into chromatin entails the wrapping of DNA around octamers of histone proteins (Olins and Olins 1974; Kornberg 1974). Further levels of packaging occur in response to numerous factors, including covalent modifications on histone tails. Histone tail modifications can influence chromatin by

modulating DNA-histone interactions or via proteins that bind to those modifications (Deuring *et al.* 2000; Corona *et al.* 2002; Carrozza *et al.* 2005). Diverse combinations of histone tail modifications provide the potential for gene regulatory information to be encoded in the chromatin fiber (Jenuwein and Allis 2001).

Actively expressed genes are often packaged with nucleosomes containing histone H3 trimethylated at Lys 36 (H3K36me3), while repressed genes are often packaged with nucleosomes containing histone H3 trimethylated at Lys 27 (H3K27me3). Studies of H3K27me3 have established several important paradigms, as summarized here. An involvement of H3K27me3 in gene repression was discovered in *Drosophila*. During *Drosophila* embryogenesis, transiently expressed transcription factors dictate which *Hox* genes are expressed and which are repressed in each body segment. A memory of *Hox* gene repression is maintained through development by Polycomb Repressive Complexes 1 and 2 (PRC1 and PRC2) (Schuettengruber *et al.* 2007). The histone methyltransferase (HMT) subunit of PRC2 that catalyzes H3K27me3 is E(z). The repressive role of E(z)/PRC2 and H3K27me3 is conserved across many species, including nematodes, mammals, and plants. A critical question is how H3K27me3 marking and repression are maintained through DNA replication and cell division, given the disassembly of nucleosomes that occurs in advance of DNA polymerase. A current well-supported model is that: 1) Parental H3/H4 histones are held near the replication fork and incorporated randomly on the two daughter chromatids. This passes H3K27me3-marked histones to daughter chromatids. 2) New histones are incorporated into daughter chromatids to restore nucleosome density. 3) H3K27me3-marked parental histones recruit PRC2 and stimulate its HMT activity to restore H3K27me3 to high levels on daughter chromatids.

This report focuses on the generation and maintenance of H3K36me3, which is less well understood than H3K27me3. H3K36me3 is conserved from yeast to humans, and is

generally associated with actively expressed genes. The paradigm that H3K36 methylation is deposited cotranscriptionally came from budding yeast, in which a single enzyme, Set2, generates all 3 levels of methylation (me1, me2, and me3). Set2 has a Set2 Rpb1 Interacting (SRI) domain through which it associates with the C terminal domain of RNA Polymerase II to deposit H3K36me in the body of genes during transcription elongation (Strahl *et al.* 2002; Kizer *et al.* 2005). The discovery that multicellular organisms have multiple H3K36 HMTs (e.g. 2 in *C. elegans*, 2 in *Drosophila*, and 4 in mammals) raises the question whether there has been diversification of the activities and functions of H3K36 HMTs (Wagner and Carpenter 2012; McDaniel and Strahl 2017). Our previous studies suggest diversification of the 2 *C. elegans* H3K36 HMTs: MET-1, like yeast Set2, generates H3K36me in a co-transcriptional manner, while MES-4 can maintain H3K36me in a manner that does not require ongoing transcription. Specifically, in *C. elegans* embryos, maternally provided MES-4 maintains H3K36me on genes that were expressed in the parental germline regardless of whether those genes are transcribed in embryos (Furuhashi *et al.* 2010; Rechtsteiner *et al.* 2010). Although MES-4 is not required in adults for germline maintenance and function, absence of maternal MES-4 in embryos causes the nascent germ cells to die (Capowski *et al.* 1991; Garvin *et al.* 1998). These findings support the following model: 1) In parental germ cells MET-1 deposits H3K36me on expressed genes during transcription. 2) In embryos MES-4 maintains H3K36me on those genes. 3) Delivery of chromosomes with H3K36me marking of germline-expressed genes to the primordial germ cells (PGCs) enables those cells to launch a proper germline transcription program.

In this study, we addressed questions raised by the model of MET-1 and MES-4 action in *C. elegans*, focusing on H3K36me3. We show that both MET-1 and MES-4 contribute to H3K36me3. To our knowledge, this is the first example of 2 different HMTs contributing to H3K36me3. The 2 HMTs differ in their temporal and spatial expression patterns in germlines and embryos and in their chromosomal targets; during germline development H3K36me3

marking of the autosomes is accomplished by both MET-1 and MES-4, while H3K36me3 marking of the X chromosomes during oogenesis is accomplished by MET-1. Both enzymes are maternally transmitted to the embryo at fertilization. Maternal MES-4 associates with sperm chromosomes soon after fertilization, and that association requires that the sperm chromosomes arrive already marked with H3K36me3. During the early embryonic cleavages, MET-1 levels rapidly diminish, while MES-4 stays high and is responsible for maintaining inherited patterns of H3K36me3. These findings support MES-4 serving a transgenerational epigenetic role to transmit gene expression information from parent germ cells to the primordial germ cells in progeny.

RESULTS

In C. elegans, H3K36me3 is generated by both MET-1 and MES-4.

MET-1-related HMTs in other organisms, Set2 in *Drosophila* and SETD2 in mammals, are thought to be fully responsible for H3K36me3 (Wagner and Carpenter 2012). However, previous immunostaining results suggested that both MET-1 and MES-4 contribute to H3K36me3 in *C. elegans*: the level of H3K36me3 immunostaining in embryos is high in wild-type, reduced in *met-1* mutants, reduced in *mes-4* mutants, and undetectable in double *met-1; mes-4* mutants (Furuhashi *et al.* 2010; Rechtsteiner *et al.* 2010). To test by an independent method if an enzyme other than MET-1 contributes to H3K36me3, we performed mass spectrometric analysis of H3 tails from wild-type and *met-1* mutant embryos. Embryos bearing either of two mutant alleles of *met-1* had robust levels of H3K36me3, which must be generated by a different HMT. MES-4 is the only other H3K36 HMT identified in *C. elegans* to date (Figure 2-1A). We could not analyze *mes-4* mutant embryos or *mes-4; met-1* double mutant embryos, because the maternal-effect sterility of those strains prevented us from collecting sufficient quantities of those mutant embryos for mass spectrometry. In combination with our immunostaining analysis (Figure 1-1), in which H3K36me3 is present in

met-1 mutants but not detectable in *met-1;mes-4* double mutants, our mass spectrometry results support MES-4 contributing to H3K36me3 on both H3.1 and variant H3.3.

In germ cells, both MET-1 and MES-4 generate H3K36me3 on the autosomes at all stages, and MET-1 additionally generates H3K36me3 on the X chromosomes in late oogenesis.

To determine the spatial and temporal pattern of H3K36me3 during germ cell development, we analyzed the distribution of H3K36me3 in germlines and gametes. Immunostaining of dissected germlines revealed chromosome-associated H3K36me3 signal in all germ nuclei, including mitotic and meiotic germ cells and mature oocytes (Figure 2-1B and 2-1C). Consistent with previous findings that the X chromosomes are transcriptionally repressed in the germline (Reinke *et al.* 2000; Kelly *et al.* 2002; Reinke *et al.* 2004), H3K36me3 staining was observed on the autosomes but not on the X from the distal end of the mitotic zone through late pachytene. (Figure 2-1B and 2-1C). By contrast, all 6 bivalents in the oocyte, including the X bivalent, stained positively for H3K36me3 (Figure 2-1C). This is consistent with previously documented turn-on of X-linked genes at late stages of oogenesis (Kelly *et al.* 2002).

To investigate the spatial activity of MES-4 and MET-1 in the germline, we immunostained dissected germlines from *met-1* and *mes-4* mutant hermaphrodites. H3K36me3 was detected in *met-1* mutant germlines, indicating that MES-4 generates H3K36me3 throughout the germline and in sperm and oocytes (Figure 2-1B). H3K36me3 was also detected in *mes-4* mutant germlines with slightly less signal in distal mitotic region, indicating that MET-1 generates H3K36me3 throughout the germline and in sperm and oocytes, with a concentration in the meiotic pachytene region (Figure 2-1B). H3K36me3 staining of the X bivalent in oocytes was detected in *mes-4* mutant germlines but not in *met-1* mutant germlines, indicating that H3K36me3 on the X is generated by MET-1 (Figure 2-1C). These

results show that MES-4 and MET-1 each generate H3K36me3 at all germline stages, and that the X chromosomes are uniquely methylated during late oogenesis by MET-1.

met-1 mutants have a temperature-sensitive and progressive fertility defect.

mes-4 mutants have a maternal-effect sterile phenotype, while *met-1* mutants do not display sterility at the standard lab temperature of 20°C (Andersen and Horvitz 2007). Because the mutant phenotypes of many germline-active genes are enhanced at elevated temperature, we tested if *met-1* mutants display a germline phenotype at 26°C. We scored fertility of wild-type and *met-1* mutant hermaphrodites cultured at 20° and 26° for multiple generations. We observed a progressive loss of fertility among *met-1* mutants at elevated temperature. 90-100% of *met-1* mutants were sterile by the fifth generation at 26°C (Figure 2-2). Thus, *met-1* mutant worms have germline defects that progressively compromise fertility but only at elevated temperature.

H3K36me3-marked chromatin is transmitted to embryos by both sperm and oocytes.

The fertility defects observed in *met-1* and *mes-4* mutants suggest that marking of chromatin by H3K36me3 is important for germline function and propagation of the species. We demonstrated above that both MET-1 and MES-4 contribute to generating H3K36me3 in the parental germline and chromatin that is packaged into oocytes (Figure 2-1C). We tested the contribution of each gamete by generating embryos by mating maternal gametes (M) with paternal gametes (P) that were generated in a wild-type parent (+) or a *met-1;mes-4* parent (-). To determine whether H3K36me3 is transmitted to embryos on oocyte and sperm chromosomes, we immunostained 1-cell embryos in which H3K36me3 transmission was only possible maternally (M+P- embryos) through the oocyte, or paternally (M-P+ embryos) through the sperm. In 1-cell M+P- embryos generated by mating feminized mothers with *met-1; mes-4* fathers that are unable to generate H3K36me3, the sperm-delivered chromosomes were H3K36me3 negative and the oocyte-delivered chromosomes were H3K36me3 positive

(Figure 2-3A). Conversely, in 1-cell M-P+ embryos generated by mating wild-type fathers with *met-1; mes-4* mothers that are unable to generate H3K36me3, the oocyte-delivered chromosomes were H3K36me3 negative and the sperm-delivered chromosomes were H3K36me3 positive (Figure 2-3B). These findings reveal that both gametes, oocytes and sperm, transmit H3K36me3-marked chromatin from the parental germline to the 1-cell embryo.

Maternal MES-4 ensures that H3K36me3 marking in embryos persists beyond the 4-cell stage.

We previously reported that MET-1 is a transcription-coupled H3K36 HMT capable of *de novo* methylation and that MES-4 is a transcription-independent H3K36 HMT devoted to maintenance of that mark (Bender *et al.* 2006; Furuhashi *et al.* 2010; Rechtsteiner *et al.* 2010). Since the germ cells in early embryos are largely transcriptionally silent {Seydoux:1997tl, Nakamura:2010ki, Spencer:2011dk}, we predicted that MES-4 and not MET-1 would be critical for maintaining H3K36me3 in early embryos. To test that prediction, we generated embryos that inherited H3K36me3 marked chromosomes but either no MES-4 or no MET-1, and analyzed levels of chromosomal H3K36me3 at progressively later stages of embryogenesis. To eliminate MES-4, we used *mes-4* M-Z- mutant embryos that lack maternally loaded MES-4 (M-) and are unable to produce zygotic MES-4 (Z-). These embryos inherited MET-1-generated H3K36me3. We quantified the intensity of H3K36me3 staining during prometaphase in 1-cell to 8-cell stage embryos. For each genotype, we compared the average intensity in single diploid nuclei of 2-, 4-, and 8-cell embryos to the average intensity in the two juxtaposed haploid pronuclei in 1-cell embryos. Staining of wild-type embryos revealed that the average intensity decreased from the 1-cell stage (set to 100%) to the 2-cell stage (71%), 4-cell stage (59%) and 8-cell stage (42%) (Figure 2-4A and 2-4B). In *mes-4* M-Z- embryos that lacked MES-4, the decrease was more rapid, dropping from the 1-cell stage (set to 100%) to the 2-cell stage (25%) and 4-cell stage (5%); staining was undetectable by

the 8-cell stage (0%) (Figure 2-4A and 2-4B). In contrast, *met-1* mutant embryos had H3K36me3 levels that were similar to or slightly higher than wild-type controls. Therefore, MES-4 but not MET-1 is required to maintain wild-type levels of H3K36me3 through the early embryonic divisions and to ensure that H3K36me3 marking persists beyond the 4-cell stage.

We noted that the rate of H3K36me3 loss in *mes-4* M-Z- embryos was greater than expected if the parental load of H3K36me3 was simply being diluted by rounds of DNA replication. Loss by dilution at each round of DNA replication would predict a drop of 50% at each subsequent stage, i.e. 100% at the 1-cell stage, then 50%, 25%, and 12.5% in each nucleus at the 2-cell, 4-cell, and 8-cell stage, respectively (Figure 2-4B). Because we observed a 75% reduction between the 1-cell and 2-cell stages in *mes-4* M-Z- embryos, we considered the possibility that H3K36me3 removal is an active process involving demethylation (Figure 2-4A and 2-4B). Two different demethylases have been reported to target H3K36me3 in *C. elegans*, JMJD-2 and JHDM-1. If JMJD-2 and/or JHDM-1 demethylate H3K36 in early embryos, we predicted that H3K36me3 levels would be higher in *jmjd-2; jhdm-1; mes-4* M-Z- embryos than in *mes-4* M-Z- embryos. We did not observe a difference between H3K36me3 levels in *jmjd-2; jhdm-1; mes-4* M-Z- embryos compared to *mes-4* M-Z- embryos (Figure 2-4B). These results suggest that the dramatic drop in H3K36me3 in *mes-4* mutant embryos is not due to demethylation by JMJD-2 or JHDM-1. Another demethylase(s) may be involved, or histone exchange may deplete H3K36me3.

MET-1 and MES-4 are maternally supplied to embryos, and MES-4 is the major HMT in early embryos.

Immunostaining wild-type germlines for MES-4 and MET-1 revealed different protein accumulation patterns (Figure 2-5A). Whereas MES-4 is enriched in the distal mitotic region and late pachytene, MET-1 is low in the distal mitotic region, increases in the mid-pachytene region, and drops again during later pachytene.

Considering the rapid loss of inherited H3K36me3 patterns in embryos lacking MES-4, we sought to determine if MET-1 and MES-4 proteins are also transmitted from the germline to embryos through the gametes. We detected immunostaining of both proteins in 1-cell embryos from wild-type hermaphrodites (Figure 2-5B) but not in 1-cell embryos from *met-1* or *mes-4* mutant mothers mated to wild-type males (Figure 2-5B). Nucleoplasmic MET-1 staining can be seen in the wild-type condition, whereas only background staining can be seen in the *met-1* M-P+ condition. These results demonstrate that all detectable MET-1 and MES-4 present in 1-cell embryos is maternally supplied via the oocyte or translated from maternal transcripts. The results further demonstrate that MES-4 staining of sperm chromosomes in 1-cell embryos is due to de novo recruitment of maternal MES-4 to incoming sperm chromosomes. This is an interesting contrast to the results above, which demonstrated that both gametes transmit H3K36me3 to embryos.

Despite the presence of both MET-1 and MES-4 at the 1-cell stage, they display different dynamics as embryogenesis proceeds. MET-1 is nucleoplasmic and the level of staining diminishes rapidly over the first few embryonic divisions, whereas MES-4 is enriched on condensed chromosomes and the levels remain relatively high through the early embryonic divisions (Figure 2-5C). This observation fits well with previously published data (Schauer and Wood 1990; Baugh *et al.* 2003) and our proposed model that maternal MES-4 is a maintenance enzyme for H3K36me3 in early embryos, while MET-1 is a transcription-coupled HMT and is unlikely to be active before global activation of the zygotic genome at the ~30-cell stage.

Maternally supplied MES-4 associates with sperm-inherited chromosomes soon after fertilization, and that association depends on their prior marking with H3K36me3.

Previous chromatin immunoprecipitation studies in *C. elegans* embryos revealed that MES-4 associates with many genes that lack RNA Polymerase II but were transcribed in parental germlines. This pattern differs from the traditional view that H3K36 HMTs are recruited to genes by elongating RNA Polymerase II. We hypothesized that maternally provided MES-4 is instead recruited to target genes in early embryos by associating with the chromatin modification that it generates, H3K36me3. We tested this possibility by taking advantage of the de novo association of maternally provided MES-4 with sperm chromosomes in wild-type 1-cell embryos. If H3K36me3 is required for this de novo association, then sperm chromosomes lacking H3K36me3 should fail to recruit maternal MES-4. We mated feminized mothers with *met-1; mes-4* fathers to generate M+P- embryos in which the oocyte-contributed chromosomes possessed H3K36me3 and the sperm-contributed chromosomes lacked H3K36me3. We did not detect MES-4 on the sperm-contributed chromosomes, which lacked H3K36me3, whereas MES-4 was highly enriched on the oocyte-contributed chromosomes, which were inherited with H3K36me3 marking (Figure 2-6A). In these M+P- 1-cell embryos, we observed nucleoplasmic MES-4 along with the H3K36me3-negative chromosomes in the sperm pronucleus, so we can rule out the possibility that maternal MES-4 was not imported into the sperm pronucleus (Figure 2-6A). These findings show that after fertilization maternal MES-4 is imported into the sperm pronucleus and associates with sperm chromosomes in a manner that requires their prior methylation on H3K36.

We wondered if the source or context of methylation of H3K36 on sperm chromosomes matters for MES-4 recruitment. To test this, we generated 1-cell embryos that inherited sperm chromosomes carrying H3K36me3 generated by only MET-1 or only MES-4 by crossing feminized worms to *mes-4* or *met-1* males, respectively. In both cases, MES-4 staining was observed on sperm chromosomes, indicating that H3K36me3 generated by either HMT is sufficient to recruit maternal MES-4 in the 1-cell embryo (Figure 2-6B). Since MES-4 is the

sole HMT for generating H3K36me2, these findings also suggest that H3K36me2 is not the critical modification for recruiting maternal MES-4 to chromosomes.

We also considered the possibility that small RNAs play a role in MES-4 recruitment to sperm chromosomes in 1-cell embryos, as a growing body of literature implicates small RNAs in transgenerational memory. Notably, the genes bound by MES-4 in embryos significantly overlap with the gene targets of the small RNAs bound by the argonaute CSR-1. To test the possibility that MES-4 recruitment to sperm chromosomes involves CSR-1, we used RNAi to deplete CSR-1 from embryos and assayed MES-4 localization by immunostaining. MES-4 chromosome association was not altered by CSR-1 depletion, suggesting that MES-4 recruitment to chromosomes in 1-cell embryos does not require CSR-1 (Figure 2-6C).

MES-4 maintains inherited patterns of H3K36me3 during early embryogenesis.
Differential marking of chromosomes by H3K36me3 and MES-4 in 1-cell M+P- embryos provides a unique opportunity to determine if inherited patterns of this histone modification persist through multiple rounds of cell division. If the distributions of histone modifications on chromosomes are transmitted through rounds of DNA replication, we would expect some of the daughter chromosomes to remain marked and some unmarked by H3K36me3 in successively later stages of embryogenesis. To test this prediction, we assessed H3K36me3 staining patterns and MES-4 localization in nuclei of M+P- embryos during each prometaphase until the 32-cell stage. The inherited pattern in these embryos was H3K36me3 and MES-4 on oocyte-contributed chromosomes and not on sperm-contributed chromosomes (Figure 2-3A). A pattern of H3K36me3 and MES-4 on only a subset of chromosomes in each nucleus was maintained until the 32-cell stage (Figure 2-7). After this stage, the nuclei were too small to assess localization of H3K36me3 and MES-4 on individual chromosomes. Because both marked and unmarked chromosomes are present in the same nuclei beginning at the 2-cell stage, the maintenance of H3K36me3 and MES-4 on only some chromosomes

suggests that the memory of H3K36me3 marking is being maintained only on those chromosomes inherited with H3K36me3. Notably, this maintenance persists until the germline founder cell P4 is born, at the 16-24-cell stage. The germ lineage is the lineage whose development and survival depend on maternal MES-4.

DISCUSSION

Recent research in the field of epigenetics suggests that gene expression information in the form of histone modifications can be transmitted not only through mitotic cell divisions, but also from parents to progeny (Hammoud *et al.* 2009a; Furuhashi *et al.* 2010; Rechtsteiner *et al.* 2010; Arico *et al.* 2011; Gaydos *et al.* 2014; Samson *et al.* 2014). This would offer organisms a mechanism to pass a memory of development and life experiences across generations. Major efforts are underway to identify what epigenetic signals are transmitted through cell divisions and from parents to progeny, which proteins are responsible for generating these signals, how signals are maintained once inherited, and for how many generations signals persist. In this study, we determined that in *C. elegans* 1) H3K36me3 is transmitted via both sperm and oocyte to progeny and through cell divisions in the early embryo, 2) two HMTs, MET-1 and MES-4, contribute to H3K36me3 in the germline and in embryos, and 3) maternally supplied MES-4 is responsible for maintaining inherited H3K36me3 in embryos. These data support the previously proposed model that epigenetic information in the form of H3K36me3 is transmitted across generations. This epigenetic information may provide a memory of which genes were expressed in the germ cells in parents and which genes should be turned on in the PGCs of progeny.

This paper focuses on H3K36me3 and the two worm HMTs that generate this modification in the adult germline and early embryo cells. The lore in the field is that in organisms with more than one H3K36 HMT, MES-4-related enzymes catalyze H3K36me2 and MET-1-related

enzymes catalyze H3K36me3. Our previous immunostaining of wild-type and mutant embryos suggested that MES-4 indeed catalyzes all H3K36me2 but that both MET-1 and MES-4 contribute to H3K36me3 (Bender *et al.* 2006; Furuhashi *et al.* 2010; Rechtsteiner *et al.* 2010). That view is supported by two findings in this paper, immunostaining of wild-type and mutant adult germlines and mass spectrometry analysis of chromatin from early embryos. The latter shows that H3K36me3 persists in the absence of MET-1, supporting the existence of at least one additional H3K36me3 HMT. MES-4 is the only other known *C. elegans* H3K36 HMT, and is of particular interest because of its unique ability to maintain methylation of H3K36 in the absence of transcription (Bender *et al.* 2006; Furuhashi *et al.* 2010; Rechtsteiner *et al.* 2010). In the absence of MET-1, H3K36me3 was detected on both H3.1 and H3.3 histone variants, suggesting that MES-4 can target both replication-dependent and replication-independent histones and could therefore propagate a memory on histones through both transcription- and replication-induced nucleosome disruption.

H3K27me3 and H3K9me2/3 are known to be propagated by a feedback loop that involves recognition of the mark by the enzyme complex that made the mark (PRC2 for H2K27me3 and SU(VAR)3-9 for H3K9me2/3) and subsequent generation of more of the same mark on nearby nucleosomes (Bannister *et al.* 2001; Margueron *et al.* 2009; Xu *et al.* 2010). Our study sheds light on the passage and maintenance of H3K36me3, a mark associated with active genes. In *C. elegans,* H3K36me3-marked chromosomes carrying a memory of gene expression from the parental germline are passed from parent to progeny via both sperm and oocyte. Once delivered to the embryo, perpetuation of marked chromosomes through the early embryonic cell divisions relies on MES-4, which is transmitted to the embryo via the oocyte and must newly associate with sperm chromosomes. That association requires that the sperm chromosomes be pre-marked with H3K36me3. Taken together these findings suggest that like transmission of H3K27me3 and H3K9me2/3, transmission of H3K36me3 involves its associated enzyme, MES-4, being recruited (directly or indirectly) to the mark it

makes. For a histone mark to provide transgenerational memory, it needs to be established in the parent, transmitted to the progeny through meiosis and gametogenesis, survive post-fertilization chromatin remodeling, and finally, be maintained during embryogenesis until the appropriate cell type is formed. Evidence for all of these steps has been reported for *C. elegans*.

In humans, despite large-scale replacement of histones with protamines during spermatogenesis, some modified histones are retained in sperm at developmentally important loci. Genes marked by H3K4me3 or H3K27me3 in sperm are correlated with expressed or silenced genes, respectively, in 4-cell embryos (Hammoud *et al.* 2009b). This result suggests histone modifications incorporated into sperm chromatin may guide gene expression patterns in the early embryos of the next generation in other organisms.

In contrast to the maintenance activity of MES-4, *C. elegans* MET-1 activity is consistent with the traditional view of H3K36me3 HMT activity being transcription-coupled. MET-1 marks the oocyte X chromosome with H3K36me3 during the late stages of oogenesis when transcription of X-linked genes is turned on. In embryos, the maternal load of MET-1 is reduced to near undetectable levels by the 8-cell stage and becomes easily detectable again around the time that zygotic transcription begins. These data are consistent with the expectations for a transcription-coupled HMT. Most transcription-coupled H3K36 HMTs contain a conserved SRI domain that mediates binding of the HMT to the C-terminal tail of elongating RNA Polymerase II. The SRI domain was first described in yeast Set2 and later in fly and mammalian homologs of Set2 (Kizer *et al.* 2005; Morris *et al.* 2005; Rebehmed *et al.* 2014). Consistent with these enzymes catalyzing H3K36me during transcription elongation, these enzymes are often localized to chromatin in the same regions of the genome as RNA Polymerase II. MET-1 contains a sequence with moderate sequence similarity to the SRI domain at a typical position (C terminal region), while MES-4 contains a sequence with only

minimal similarity to an SRI domain at an atypical position (overlapping the SET domain) (Brian Strahl, personal communication). While MET-1 may be primarily responsible for transcription-coupled H3K36me3 and perhaps involved in establishment of an epigenetic memory of active genes, it is only essential at elevated temperature.

The paradigm of heritable epigenetic repression mediated by *Drosophila* PRC2 and H3K27me3 also includes antagonism, or anti-repression, by trithorax group proteins (Kassis *et al.* 2017). The trithorax group of proteins, which includes an H3K36 HMT, protects genes from PRC2-mediated repression. In worms, MES-4 and methylated H3K36 antagonize deposition of H3K27me3 (Gaydos *et al.* 2012). *In vitro* assays demonstrate that PRC2 is unable to methylate nucleosomes with pre-existing H3K36me2 or me3 (Yuan *et al.* 2011; Schmitges *et al.* 2011). Embryos that do not receive maternal MES-4 develop into sterile adults, possibly because the memory of expressed germline genes is not delivered to the PGCs. One possible consequence of losing the memory of active genes is the encroachment of H3K27me3 and inappropriate silencing of genes required for the germline developmental program, Indeed, depletion of MES-4 from embryos leads to loss of H3K36me3 from germline genes and acquisition of H3K27me3 on those genes (Rechtsteiner *et al.* 2010). Therefore, the failure to develop a mature germline in *mes-4* mutants may be the result of inheriting an altered epigenome, silencing of genes required for germline development, and inappropriately expressing genes not normally expressed as part of the germline program.

The maintenance of gene expression patterns is required to ensure that cell fates are maintained. If cells within a tissue lose or change fate the function of that tissue may be compromised or become cancerous if cells revert to a proliferative state. A transgenerational memory that is transmitted across generations could influence not only the development of the inheriting organism, also the fitness of the species as a whole. This is an exciting possibility, and current efforts are focused on determining if environmental factors can

change the epigenome, how changes are transmitted to subsequent generations, and what the consequences inheriting changes has on the next generation. In *C. elegans*, it's clear that the MES chromatin factors function antagonistically across generations to promote germline development. It is likely that the patterns of H3K27me3 and H3K36me3 inherited by the PGCs serve to guide gene expression patterns as they do during *Drosophila* embryogenesis, but it's still unclear if and how this epigenetic memory influences gene expression in nascent germ cells.

MATERIALS AND METHODS

Strains and culture

C. elegans were maintained at 15°C or 20°C on NGM (Nematode Growth Medium) agar plates using *Escheria coli* OP50 as a food source. Experiments were carried out at 20°, 24°, or 26°. Strains used for this study include N2 (Bristol) as wild-type, DH0245 *fem-2(b245ts) III*, SS0875 *met-1(n4337) I/hT2g I; mes-4(bn73) dpy-11(e224) V/DnT1 (IV:V)*, SS1095 *mes-4(bn73) V/DnT1*-GFP *(IV;V)*, SS1139 *met-1(tm1738) I/ht2g* I, and SS1140 *met-1(n4337) I/ht2g I*. Both *met-1* mutant alleles lack any detectable MET-1 histone methyltransferase activity in immunostaining assays. *met-1(tm1738)* contains a 565 bp deletion and no protein is detectable by antibody staining. *met-1(n4337)* contains an 1,860 bp deletion and some protein is detectable using and antibody targeting an epitope in the second ORF, upstream of the SET domain.

Histone extraction

The histone extraction protocol was adapted from (Lin and Garcia 2012). Worms were grown in liquid culture and embryos collected by digesting adults with an alkaline-bleach solution (1% NaOCl in 0.5 M NaOH) and freezing embryos in liquid nitrogen for storage. Embryo populations were staged by fixing a sample of collected embryos prior with methanol prior to freezing, and imaging nuclei with DAPI. Populations were between 62% and 92% early embryo (<100 cell stage) Frozen wild-type and *met-1* mutant early embryos were thawed in 10 ml modified NPB (10 mM Tris pH 7.5, 40 mM NaCl, 90 mM KCl, 2 mM EDTA, 0.5 mM EGTA, 1 mM DTT, 0.5 mM spermidine, 0.25 mM spermine, 0.1% Triton X-100, Roche EDTA-free protease inhibitor cocktail, 10 mM sodium butyrate, 10 mM glycerolphosphate), then dounced with a glass dounce homogenizer and 30 strokes of a tight-fitting pestle to free nuclei. Nuclei were enriched by pelleting cellular debris at 100g for 2 minutes at 4°, collecting the supernatant, adjusting the volume to 45 mL with modified NPB, pelleting residual debris

at 100g for 5 minutes, and collecting the supernatant. Enriched nuclei were washed twice in modified NPB by centrifuging at 1000g for 10 minutes. Nuclei were resuspended in 400 ul 0.4 N H_2SO_4, vortexed briefly to ensure nuclei were completely resuspended, and rotated overnight at 4°. Samples were centrifuged at 16,000g for 10 min at 4° to pellet insoluble debris. The supernatants containing histones were transferred to clean tubes, and histones were precipitated by the addition of 100% TCA to a final concentration of 33%. Samples were inverted to mix and rotated overnight at 4°, then centrifuged at 16,000g for 10 min at 4°. The pellets containing histones were washed twice with 1 ml ice-cold acetone. After the second wash, the pellets allowed to air-dry for 20 min at room temperature

Mass spectrometry

Histone propionylation and digestion: Histone propionylation and digestion was performed as previously described with minor modification (Sidoli *et al.* 2016). Propionic anhydride solution was freshly prepared by mixing propionic anhydride with 2-propanol in a ratio of 1:3 (v/v) creating the propionylation mix. 15 µl of propionylation mix was added to the histone sample in the ratio of 1:2 (v/v), immediately followed by 7.5 µl of ammonium hydroxide to re-balance the pH at around 8.0. Samples were incubated for 15 minutes at 37°C. Propionylation was repeated a second time after drying samples in a speedvac centrifuge. Samples were dried and resuspended in 50 mM NH_4HCO_3 overnight at room temperature with trypsin at an enzyme:sample ratio of 1:20. After digestion, the derivatization reaction was performed again twice to derivatize peptide N-termini. Samples were desalted using C_{18} Stage-tips prior to LC-MS analysis.

NanoLC−MS/MS: Samples were analyzed by using a nanoLC-MS/MS setup. 1 µg of sample was loaded onto an in-house packed 75 µm ID x 20 cm Reprosil-Pur C18-AQ (3 µm; Dr. Maisch GmbH, Germany) nano-column using an EASY-nLC nano-HPLC (Thermo Scientific, San Jose, CA, USA). The HPLC gradient was as follows: 0% to 26% solvent B (A = 0.1%

formic acid; B = 95% acetonitrile, 0.1% formic acid) over 45 minutes, from 26% to 80% solvent B in 5 minutes, 80% B for 10 minutes at a flow-rate of 300 nL/min. nLC was coupled online with an Orbitrap Elite MS (Thermo Scientific, San Jose, CA, USA). Runs were acquired using data-independent acquisition (DIA) as described (Sidoli *et al.* 2015). Briefly, two full scan MS spectra (*m/z* 300−1100) were acquired in the orbitrap at a resolution of 120,000 (at 200 *m/z* FWHM) in between 16 MS/MS events spanning through the mass range, each acquired in the ion trap with an isolation window of 50 *m/z*. Fragmentation was performed by using collision induced dissociation (CID) set at to 35%.

Data analysis: Raw MS data were analyzed by using Skyline (MacLean *et al.* 2010) by performing extracted ion chromatography of the different modified and unmodified isoforms of the peptide of histone H3 KSAPTTGGVKKPHR (aa 27-40). MS/MS chromatographic profiles, acquired due to DIA, were used to increase the confidence on the correct signal to extract. The relative abundance of PTMs was determined by dividing the area of a particular isoform by the summed total area of all peptide isoforms.

Immunostaining

The immunostaining protocol was adapted from (Strome and Wood 1983). Gravid adult worms were dissected to isolate germlines, oocytes, and embryos. Dissections were done in drops of Egg Buffer (25mM HEPES pH 7.4, 118mM NaCl, 48mM KCl, 2mM EDTA, 5mM EGTA) on a polylysine-coated slide. After dissection, a coverslip was placed over the sample and the slide was immersed in liquid nitrogen for at least 2 min. The coverslip was removed, and the samples were fixed in methanol at 4°C for 10 min, followed by acetone at 4°C for 10 min, and then air dried.

Slides were incubated with 1.5% ovalbumin/1.5% bovine serum albumin in PBS-T (1xPBS, 0.1% Tween® 20) for 30 min at room temperature, followed by primary antibody diluted in

PBS-T overnight at 4°. Primary antibody dilutions were: 1:50,000 mouse anti-H3K36me3 (from Hiroshi Kimura), 1:20,000 mouse anti-H3K36me2 (from Hiroshi Kimura), 1:20,000 rabbit anti-MET-1 (SDI), and 1:500 rabbit anti-MES-4. Slides were washed 3x 10 min in PBS-T at room temperature for 1 hr, and then incubated with 1:300 Alexa Fluor secondary antibodies (Life Technologies) diluted in PBS-T for 2 hr at room temperature. Slides were washed 3x 10 min in PBS-T at room temperature, and mounted in Gelutol mounting fluid.

The following figures were generated using images acquired with a Volocity spinning disk confocal system (Perkin-Elmer/Improvision, Norwalk, CT, USA) fitted on a Nikon Eclipse TE2000-E inverted microscope: Figure 1B (male germlines), Figure 3B, Figure 6C (*csr-1(RNAi)*), Figure 7. All other images were acquired using the Solamere system described below.

Germlines, oocytes, and embryos were imaged with a Solamere spinning disk confocal system controlled by uManager software (Edelstein et al. 2014). The set-up was as follows: Yokogawa CSUX-1 scan head, Nikon (Garden City, NY) TE2000-E inverted stand, Hamamatsu ImageEM 32 camera, 561-nm laser, and Plan Apo 360/1.4 numerical aperture oil objective.

Germlines presented in Figure 2-5A were straightened post-acquisition using the imageJ straighten plugin (Schneider *et al.* 2012).

Quantification of immunostaining

The quantification protocol was adapted from (McCloy *et al.* 2014) and (Burgess *et al.* 2010). Images were acquired using the Volocity imaging set-up described above and used for quantification of H3K36me3 antibody staining, which was performed using the protocol and antibodies described above. All images were acquired within the linear range and analyzed in

ImageJ. In brief, a region was drawn around chromosomes using the DAPI channel, then the integrated density (intensity) of H3K36me3 signal within the region was measured. Background was determined by measuring the intensity of 3 circular spots outside of the nucleus and averaging their intensity. The background normalized intensity measurement used for analysis was the intensity of the H3K36me3 signal – (area of selected region * the average background intensity).

Analysis of fertility

To score fertility at 20°, wild-type or homozygous *met-1* L4s for each generation (F1 through F5) were selected to be scored to avoid biased selection of fertile or sterile worms. Worms were visually scored ~24 hours later using a Leica M80 stereo microscope. Worms with embryos were scored as fertile and worms without embryos were scored as sterile. Worms that weren't obviously fertile or sterile were cloned onto individual plates and scored as fertile if they laid embryos, and sterile if they did not. Fertile homozygous *met-1* mutants were chosen from each generation to produce progeny to score in the next generation. To score fertility at 26°, wild-type L4s were shifted from 20° to 26° and L4 F1 progeny were selected for scoring ~24 hours later. Wild-type worms were continually passaged at 26°, and generations F2-F5 were scored by selecting L4s to avoid selection bias. *met-1* heterozygous L4s were shifted from 20° to 26°, and homozygous L4 F1 progeny were selected for scoring ~24 hours later. Homozygous *met-1* worms were continually passaged at 26°, and generations F2-F5 were scored by selecting L4s to avoid selection bias.

RNAi depletion of CSR-1, EGO-1, and DRH-3

N2 hermaphrodites were fed bacteria expressing dsRNA against *csr-1, ego-1,* and *drh-3* (from the Ahringer RNAi feeding library (Kamath and Ahringer 2003)). To generate *csr-1(RNAi)* embryos, N2 hermaphrodites were placed on RNAi feeding plates as synchronized L1s and cultured at 24° until they started producing embryos.

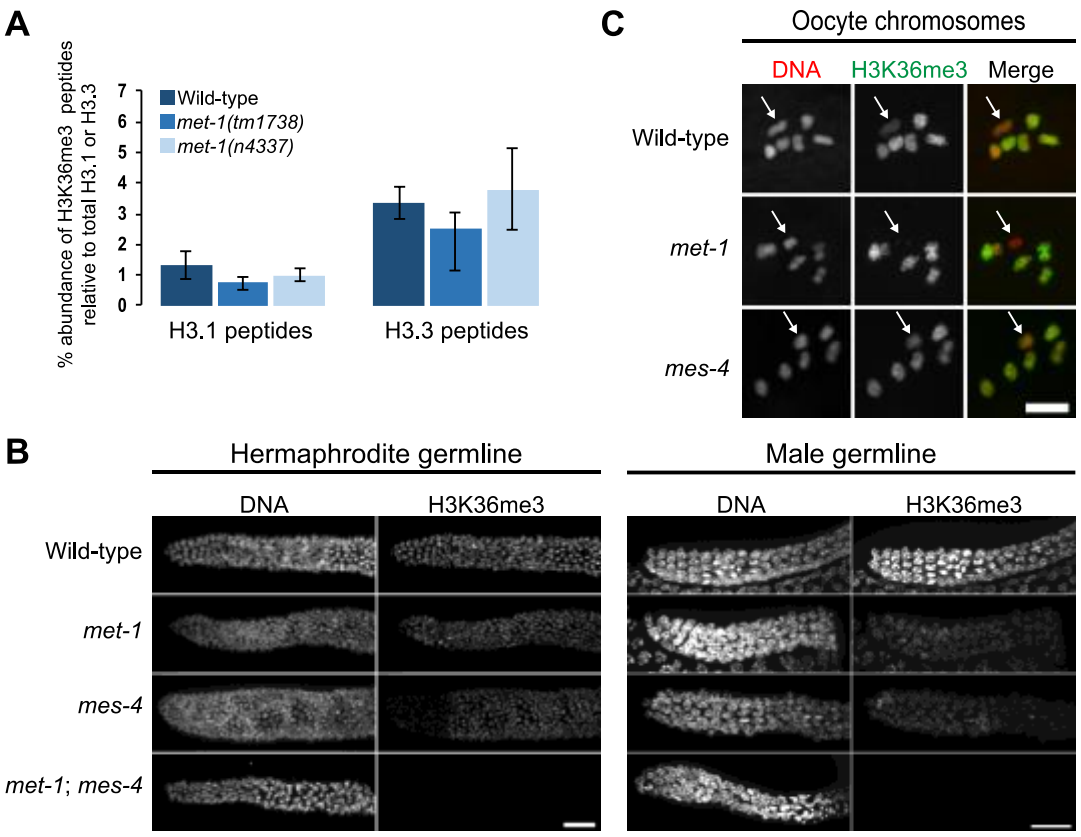

Figure 2-1 H3K36me3 is generated by both MET-1 and MES-4 in germlines and embryos, but MET-1 is solely responsible for H3K36me3 on the oocyte X chromosome. (A) Relative abundance of H3.1K36me3 and H3.3K36me3 peptide fragments from wild-type, *met-1(tm1738)*, and *met-1(n4337)* embryonic nuclei, as determined by mass spectrometry. Percent abundance is relative to total H3.1 or H3.3 peptides detected. Error bars represent SEM. (B) Immunofluorescence images showing DNA and H3K36me3 in distal germlines from wild-type, *met-1(n4337)*, *mes-4(bn73)*, and *met-1(n4337)*; *mes-4(bn73)* adult hermaphrodites and males. Scale bar, 20 um. (C) Immunofluorescence images showing DNA (red) and H3K36me3 (green) on oocyte chromosomes from wild-type, *met-1(n4337)*, and *mes-4(bn73)* hermaphrodites. White arrow indicates the X chromosome bivalent. Scale bar, 20 um.

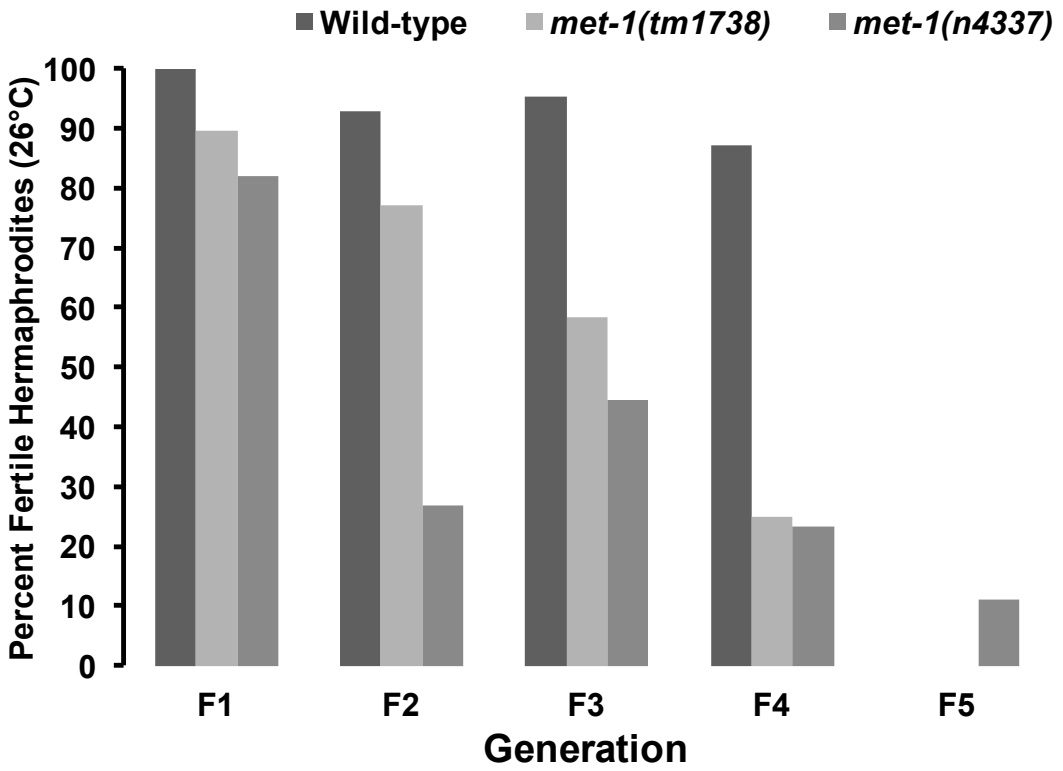

Figure 2-2 *met-1* mutants become progressively sterile when cultured at elevated temperature. Percent fertility in each generation of wild-type and *met-1* mutants maintained and scored at 26°. No F5 *met-1(tm1738)* worms were fertile. No F5 wild-type worms were scored.

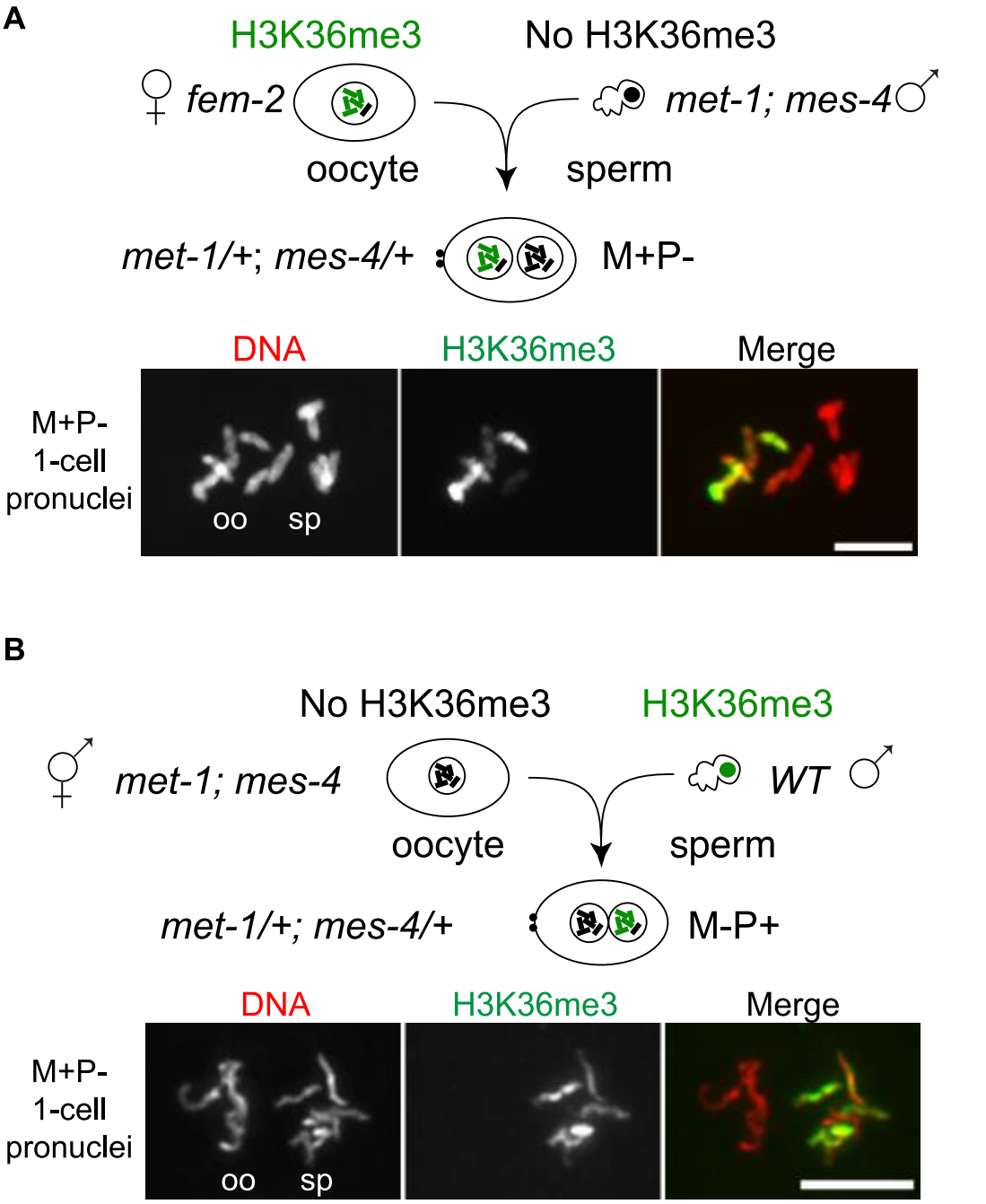

Figure 2-3 Oocytes and sperm transmit H3K36me3-marked chromosomes to the embryo. (A) Immunofluorescence image of DNA (red) and H3K36me3 (green) prometaphase chromosomes in 1-cell M+P- embryo from *met-1(n4337)*; *mes-4(bn73)* males mated to *fem-2* females. Oocyte-derived (oo) and sperm-derived (sp) chromosomes were identified by their position relative to the polar bodies (not shown). (B) Immunofluorescence image of DNA (red) and H3K36me3 (green) prometaphase chromosomes in 1-cell M-P+ embryo from wild-type males mated to *met-1(n4337); mes-4(bn73)* females. Scale bar, 5 um. (M) Maternal supply of gene product. (Z) Zygotic synthesis of gene product.

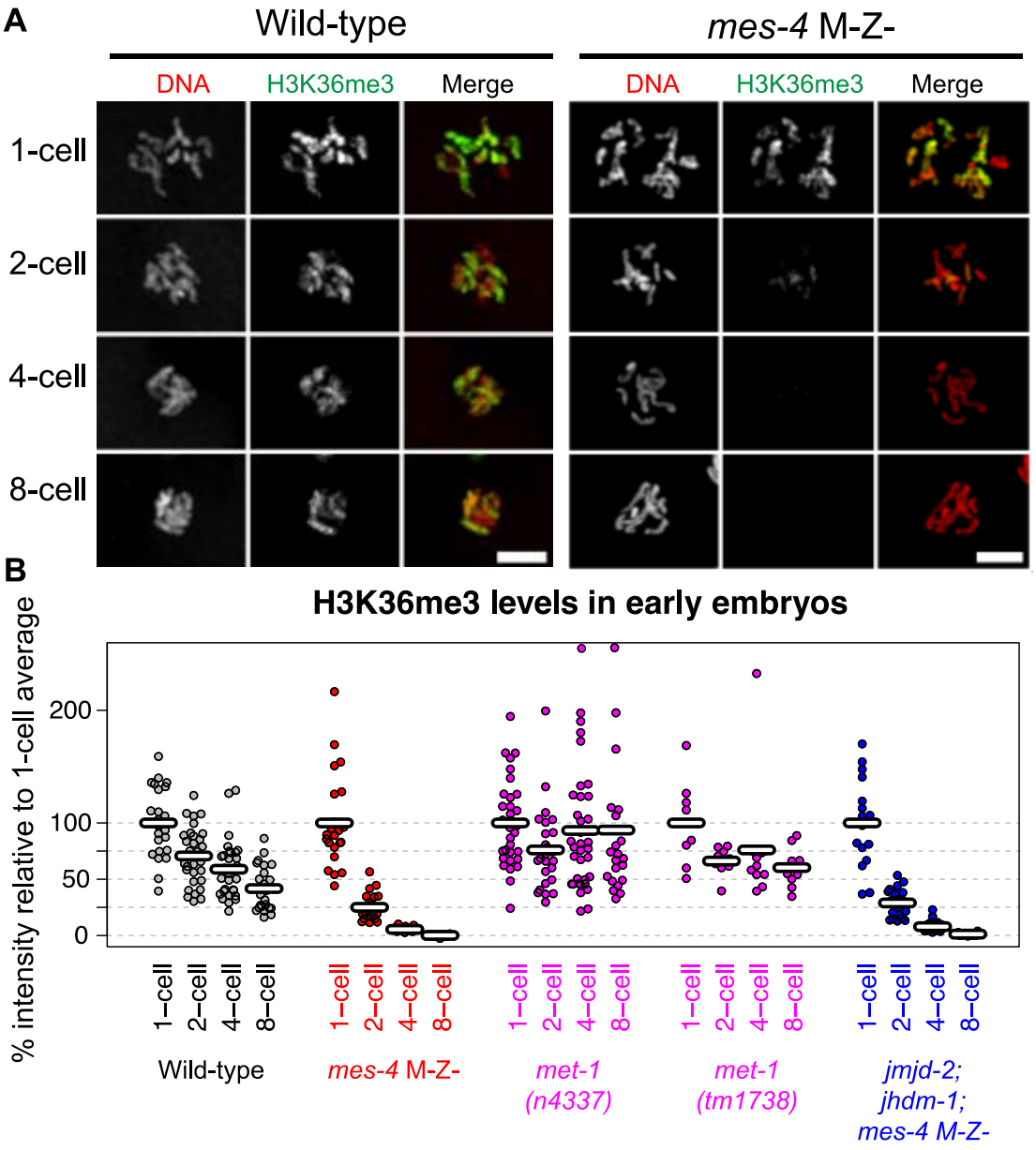

Figure 2-4 MES-4, but not MET-1, maintains H3K36me3 through cell division in early embryos. (A) Immunofluorescence images of DNA (red) and H3K36me3 (green) in nuclei from wild-type and M-Z- *mes-4(bn73)* embryos. Scale bar, 5 um. (B) Quantification of nuclear H3K36me3 immunofluorescence intensity in single nuclei of wild-type, *mes-4(bn73)* mutant, *met-1* mutant, and *jmjd-2(tm2966)*; *jhdm-1(tm2918)*; *mes-4(bn73)* triple mutant embryos. For each genotype, percent intensity is relative to the average intensity of 1-cell nuclei, which was set to 100%. Each point represents an individual nucleus. Horizontal marks represent the mean. The two upper-most points in *met-1(n4337)* 4-cell and 8-cell were 293% and 399%, respectively, but were placed within the scale shown in order to display details for the majority of data points. (M) Maternal supply of gene product. (Z) Zygotic synthesis of gene product.

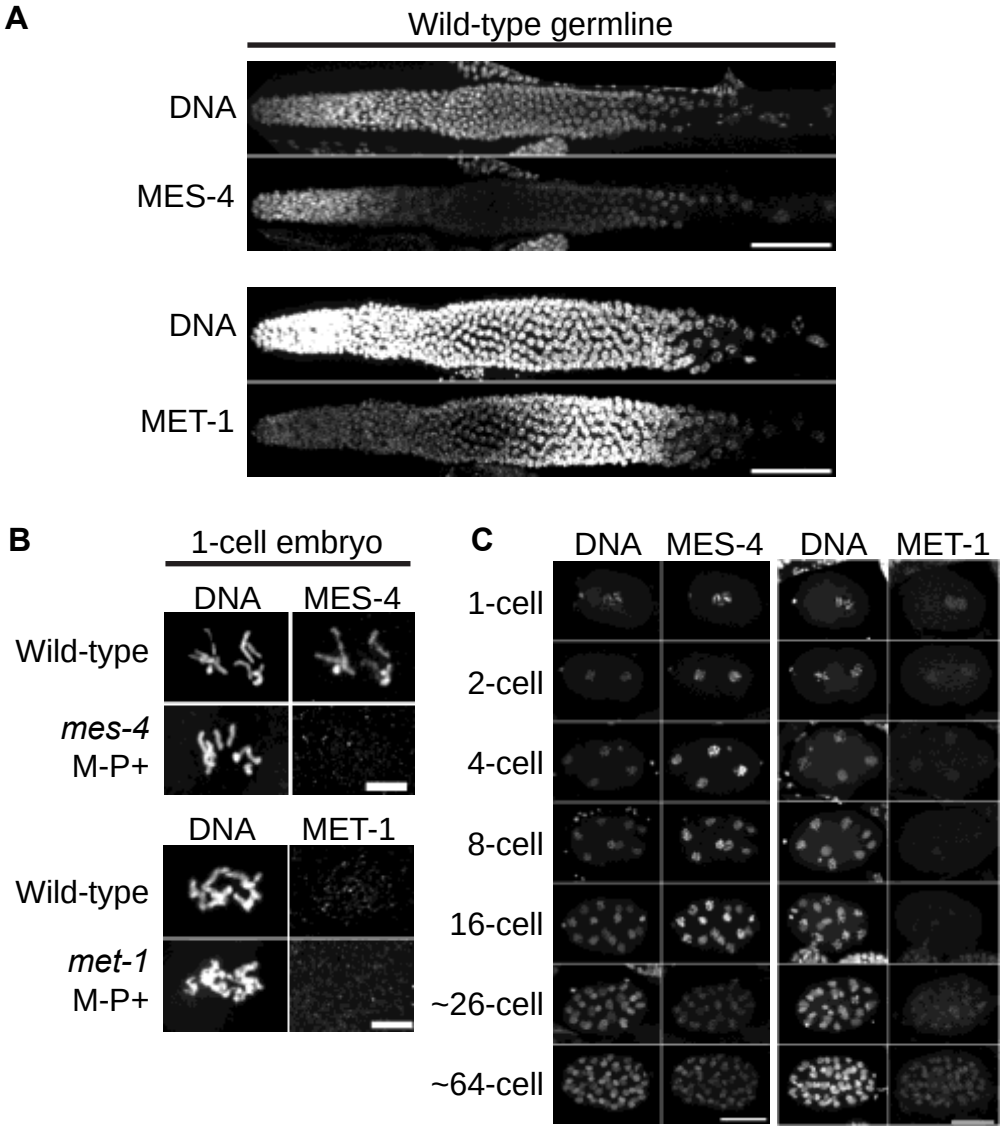

Figure 2-5 MET-1 and MES-4 have different spatial and temporal expression patterns in germlines and embryos. (A) Immunofluorescence images showing DNA and MET-1 or MES-4 in wild-type hermaphrodite germlines. Germline images are oriented with distal germline to the left and late pachytene to the right. Scale bar, 50 um. (B) Immunofluorescence images of 1-cell embryos showing DNA and the maternal contribution (wild-type) or paternal contribution (*mes-4(bn73)* M-P+, *met-1(tm1738)* M-P+) of MES-4 or MET-1. Scale bar, 10 um (C) Immunofluorescence images showing DNA and MES-4 or MET-1 in wild-type embryos. Scale bar, 20 um. (M) Maternal supply of gene product. (P) Paternal supply of gene product.

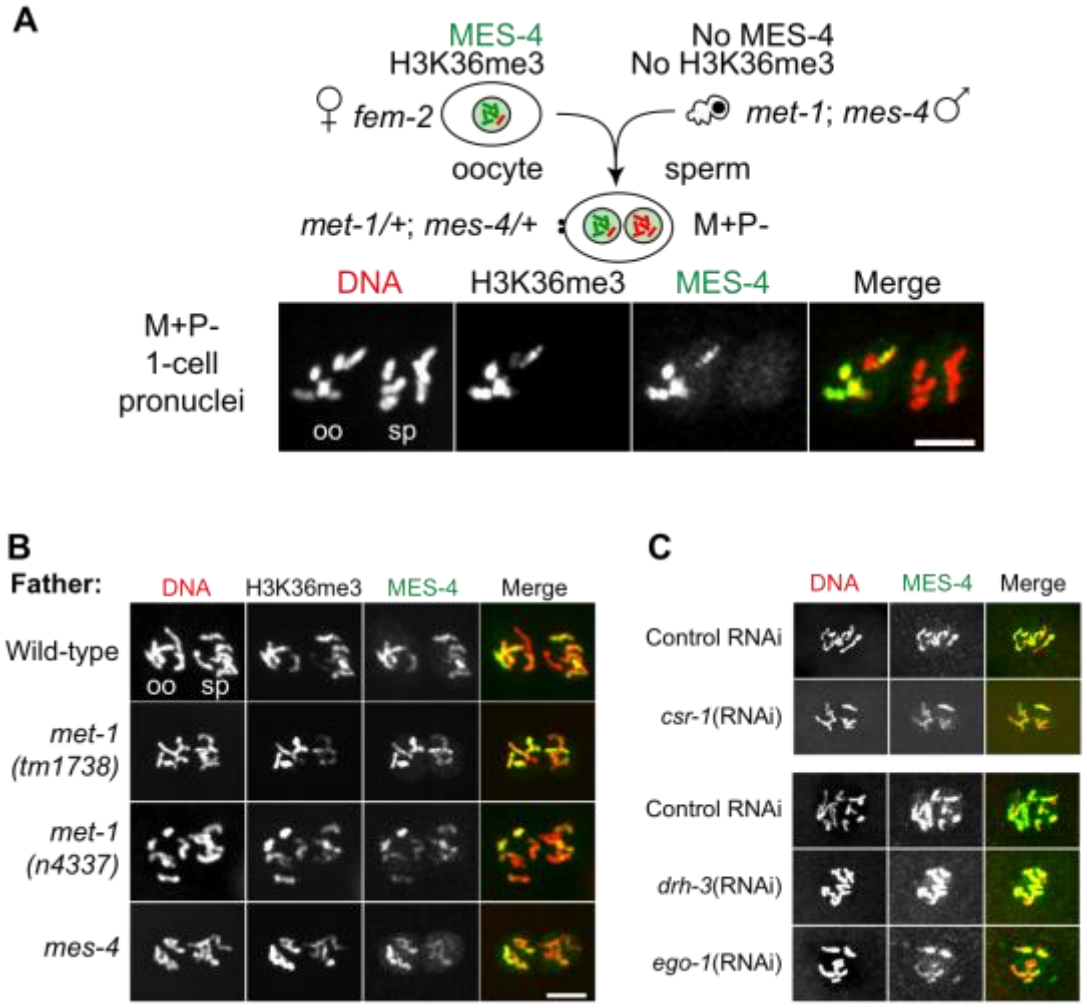

Figure 2-6 Recruitment of maternally supplied MES-4 to sperm chromosomes requires H3K36me3 generated by either MET-1 or MES-4 and is independent of small RNAs. (A) Immunofluorescence images showing DNA (red), H3K36me3, and MES-4 (green) staining on prometaphase chromosomes in 1-cell M+P- embryos from *met-1(n4337)*; *mes-4(bn73)* males mated to *fem-2* females. Brightness and contrast were enhanced to highlight nucleoplasmic MES-4. Oocyte-derived (oo) and sperm-derived (sp) chromosomes. Scale bar, 5 um. (B) Immunofluorescence images showing DNA (red), H3K36me3, and MES-4 (green) staining on prometaphase chromosomes in 1-cell embryos from wild-type hermaphrodites, *mes-4(bn73)* males mated to *fem-2* females, or *met-1* males mated to *fem-2* females. Embryos from wild-type fathers contain paternal chromosomes carrying H3K36me3 generated by MET-1 and MES-4. Embryos from *met-1* fathers contain paternal chromosomes carrying H3K36me3 generated by only MES-4. Embryos from *mes-4* fathers contain paternal chromosomes carrying H3K36me3 generated by only MET-1. Scale bar, 5 um. (C) Immunofluorescence images showing DNA (red) and MES-4 (green) staining on prometaphase chromosomes in 1-cell embryos from RNAi treated hermaphrodites. (M) Maternal supply of gene product. (P) Paternal supply of gene product.

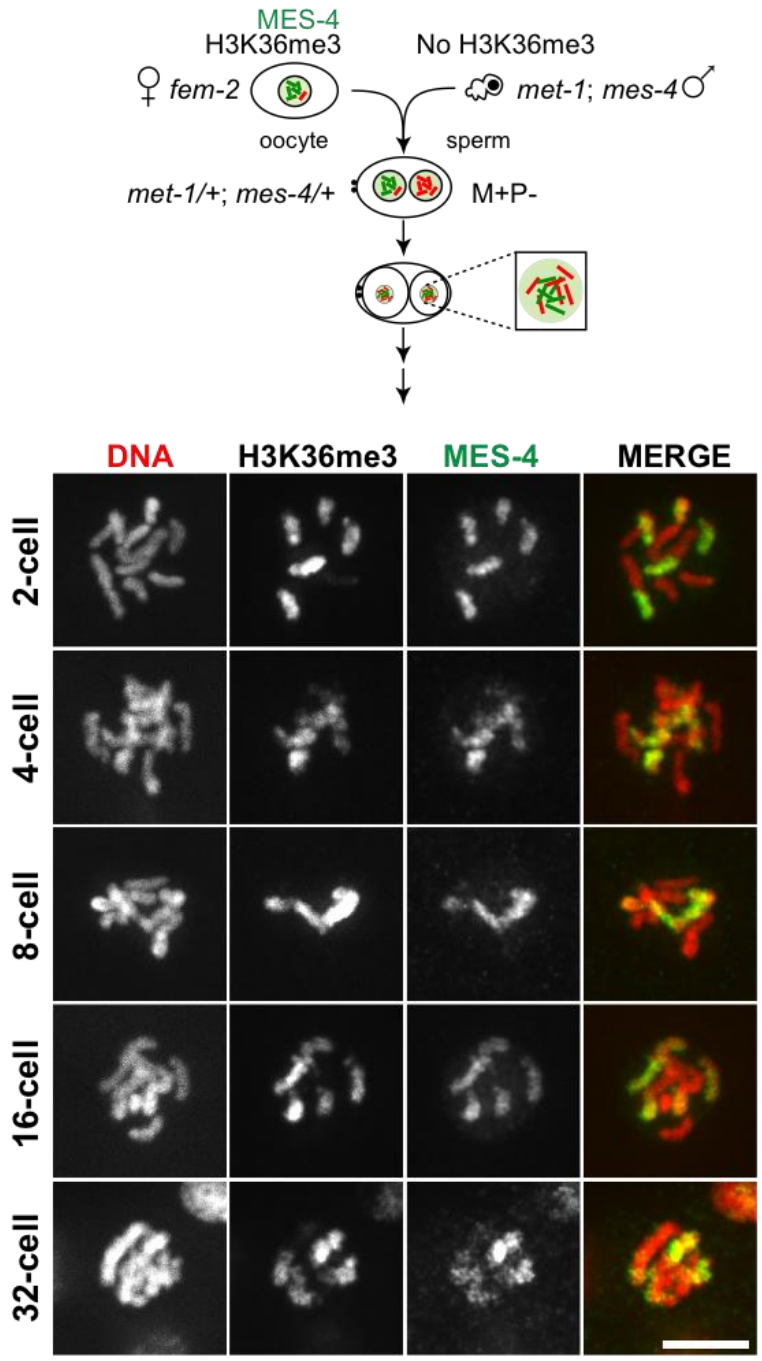

Figure 2-7 MES-4 maintains H3K36me3 on a subset of chromosomes, likely those that entered the embryo with pre-existing H3K36me3. Immunofluorescence images of DNA (red), H3K36me3, and MES-4 (green) on prometaphase chromosomes in single nuclei of M+P- embryos from *met-1(n4337)*; *mes-4(bn73)* males mated to fem-2 females. Scale bar, 5 um. (M) Maternal supply of gene product. (P) Paternal supply of gene product.

REFERENCES

Andersen E. C., Horvitz H. R., 2007 Two C. elegans histone methyltransferases repress lin-3 EGF transcription to inhibit vulval development. Development **134**: 2991–2999.

Arico J. K., Katz D. J., van der Vlag J., Kelly W. G., 2011 Epigenetic patterns maintained in early Caenorhabditis elegans embryos can be established by gene activity in the parental germ cells. (JT Lee, Ed.). PLoS Genet **7**: e1001391.

Bannister A. J., Kouzarides T., 2011 Regulation of chromatin by histone modifications. Cell Res. **21**: 381–395.

Bannister A. J., Zegerman P., Partridge J. F., Miska E. A., Thomas J. O., Allshire R. C., Kouzarides T., 2001 Selective recognition of methylated lysine 9 on histone H3 by the HP1 chromo domain. Nature **410**: 120–124.

Barski A., Cuddapah S., Cui K., Roh T.-Y., Schones D. E., Wang Z., Wei G., Chepelev I., Zhao K., 2007 High-resolution profiling of histone methylations in the human genome. Cell **129**: 823–837.

Baugh L. R., Hill A. A., Slonim D. K., Brown E. L., Hunter C. P., 2003 Composition and dynamics of the Caenorhabditis elegans early embryonic transcriptome. Development **130**: 889–900.

Bell O., Conrad T., Kind J., Wirbelauer C., Akhtar A., Schübeler D., 2008 Transcription-coupled methylation of histone H3 at lysine 36 regulates dosage compensation by enhancing recruitment of the MSL complex in Drosophila melanogaster. Mol. Cell. Biol. **28**: 3401–3409.

Bell O., Wirbelauer C., Hild M., Scharf A. N., Schwaiger M., MacAlpine D. M., Zilbermann F., van Leeuwen F., Bell S. P., Imhof A., Garza D., Peters A. H., Schübeler D., 2007 Localized H3K36 methylation states define histone H4K16 acetylation during transcriptional elongation in Drosophila. The EMBO Journal **26**: 4974–4984.

Bender L. B., Suh J., Carroll C. R., Fong Y., Fingerman I. M., Briggs S. D., Cao R., Zhang Y., Reinke V., Strome S., 2006 MES-4: an autosome-associated histone methyltransferase that participates in silencing the X chromosomes in the C. elegans germ line. Development **133**: 3907–3917.

Burgess A., Vigneron S., Brioudes E., Labbé J.-C., Lorca T., Castro A., 2010 Loss of human Greatwall results in G2 arrest and multiple mitotic defects due to deregulation of the cyclin B-Cdc2/PP2A balance. Proc. Natl. Acad. Sci. U.S.A. **107**: 12564–12569.

Capowski E. E., Martin P., Garvin C., Strome S., 1991 Identification of grandchildless loci whose products are required for normal germ-line development in the nematode Caenorhabditis elegans. Genetics **129**: 1061–1072.

Carrozza M. J., Li B., Florens L., Suganuma T., Swanson S. K., Lee K. K., Shia W.-J., Anderson S., Yates J., Washburn M. P., Workman J. L., 2005 Histone H3 methylation by Set2 directs deacetylation of coding regions by Rpd3S to suppress spurious intragenic transcription. Cell **123**: 581–592.

Corona D. F. V., Clapier C. R., Becker P. B., Tamkun J. W., 2002 Modulation of ISWI function by site-specific histone acetylation. EMBO Rep. **3**: 242–247.

Deuring R., Fanti L., Armstrong J. A., Sarte M., Papoulas O., Prestel M., Daubresse G., Verardo M., Moseley S. L., Berloco M., Tsukiyama T., Wu C., Pimpinelli S., Tamkun J. W., 2000 The ISWI chromatin-remodeling protein is required for gene expression and the maintenance of higher order chromatin structure in vivo. Mol. Cell **5**: 355–365.

Dorighi K. M., Tamkun J. W., 2013 The trithorax group proteins Kismet and ASH1 promote H3K36 dimethylation to counteract Polycomb group repression in Drosophila. Development **140**: 4182–4192.

Ebert A., Lein S., Schotta G., Reuter G., 2006 Histone modification and the control of heterochromatic gene silencing in Drosophila. Chromosome Res **14**: 377–392.

Furuhashi H., Takasaki T., Rechtsteiner A., Li T., Kimura H., Checchi P. M., Strome S., Kelly W. G., 2010 Trans-generational epigenetic regulation of C. elegans primordial germ cells. Epigenetics Chromatin **3**: 15.

Garvin C., Holdeman R., Strome S., 1998 The phenotype of mes-2, mes-3, mes-4 and mes-6, maternal-effect genes required for survival of the germline in Caenorhabditis elegans, is sensitive to chromosome dosage. Genetics **148**: 167–185.

Gaydos L. J., Rechtsteiner A., Egelhofer T. A., Carroll C. R., Strome S., 2012 Antagonism between MES-4 and Polycomb repressive complex 2 promotes appropriate gene expression in C. elegans germ cells. Cell Rep **2**: 1169–1177.

Gaydos L. J., Wang W., Strome S., 2014 Gene repression. H3K27me and PRC2 transmit a memory of repression across generations and during development. Science **345**: 1515–1518.

Gerstein M. B., Lu Z. J., Van Nostrand E. L., Cheng C., Arshinoff B. I., Liu T., Yip K. Y., Robilotto R., Rechtsteiner A., Ikegami K., Alves P., Chateigner A., Perry M., Morris M., Auerbach R. K., Feng X., Leng J., Vielle A., Niu W., Rhrissorrakrai K., Agarwal A., Alexander R. P., Barber G., Brdlik C. M., Brennan J., Brouillet J. J., Carr A., Cheung M.-S., Clawson H., Contrino S., Dannenberg L. O., Dernburg A. F., Desai A., Dick L., Dosé A. C., Du J., Egelhofer T., Ercan S., Euskirchen G., Ewing B., Feingold E. A., Gassmann R., Good P. J., Green P., Gullier F., Gutwein M., Guyer M. S., Habegger L., Han T., Henikoff J. G., Henz S. R., Hinrichs A., Holster H., Hyman T., Iniguez A. L., Janette J., Jensen M., Kato M., Kent W. J., Kephart E., Khivansara V., Khurana E., Kim J. K., Kolasinska-Zwierz P., Lai E. C., Latorre I., Leahey A., Lewis S., Lloyd P., Lochovsky L., Lowdon R. F., Lubling Y., Lyne R., MacCoss M., Mackowiak S. D., Mangone M., McKay S., Mecenas D., Merrihew G., Miller D. M., Muroyama A., Murray J. I., Ooi S.-L., Pham H., Phippen T., Preston E. A., Rajewsky N., Rätsch G., Rosenbaum H., Rozowsky J., Rutherford K., Ruzanov P., Sarov M., Sasidharan R., Sboner A., Scheid P., Segal E., Shin H., Shou C., Slack F. J., Slightam C., Smith R., Spencer W. C., Stinson E. O., Taing S., Takasaki T., Vafeados D., Voronina K., Wang G., Washington N. L., Whittle C. M., Wu B., Yan K.-K., Zeller G., Zha Z., Zhong M., Zhou X., modENCODE Consortium, Ahringer J., Strome S., Gunsalus K. C., Micklem G., Liu X. S., Reinke V., Kim S. K., Hillier L. W., Henikoff S., Piano F., Snyder M., Stein L., Lieb J. D., Waterston R. H., 2010 Integrative analysis of the Caenorhabditis elegans genome by the modENCODE project. Science **330**: 1775–1787.

Grewal S. I. S., Elgin S. C. R., 2002 Heterochromatin: new possibilities for the inheritance of structure. Current Opinion in Genetics & Development **12**: 178–187.

Hammoud S. S., Nix D. A., Zhang H., Purwar J., Carrell D. T., Cairns B. R., 2009a Distinctive Chromatin in Human Sperm Packages Genes for Embryo Development. Nature **460**: 473–478.

Hammoud S. S., Nix D. A., Zhang H., Purwar J., Carrell D. T., Cairns B. R., 2009b Distinctive chromatin in human sperm packages genes for embryo development. Nature **460**: 473–478.

Jenuwein T., Allis C. D., 2001 Translating the histone code. Science **293**: 1074–1080.

Kamath R. S., Ahringer J., 2003 Genome-wide RNAi screening in Caenorhabditis elegans. Methods **30**: 313–321.

Kassis J. A., Kennison J. A., Tamkun J. W., 2017 Polycomb and Trithorax Group Genes in Drosophila. Genetics **206**: 1699–1725.

Kelly W. G., Schaner C. E., Dernburg A. F., Lee M.-H., Kim S. K., Villeneuve A. M., Reinke V., 2002 X-chromosome silencing in the germline of C. elegans. Development **129**: 479–492.

Kizer K. O., Phatnani H. P., Shibata Y., Hall H., Greenleaf A. L., Strahl B. D., 2005 A novel domain in Set2 mediates RNA polymerase II interaction and couples histone H3 K36 methylation with transcript elongation. Mol. Cell. Biol. **25**: 3305–3316.

Kornberg R. D., 1974 Chromatin Structure: A Repeating Unit of Histones and DNA. Science **184**: 868–871.

Krogan N. J., Kim M., Tong A., Golshani A., Cagney G., Canadien V., Richards D. P., Beattie B. K., Emili A., Boone C., Shilatifard A., Buratowski S., Greenblatt J., 2003 Methylation of histone H3 by Set2 in Saccharomyces cerevisiae is linked to transcriptional elongation by RNA polymerase II. Mol. Cell. Biol. **23**: 4207–4218.

Lanzuolo C., Sardo Lo F., Diamantini A., Orlando V., 2011 PcG complexes set the stage for epigenetic inheritance of gene silencing in early S phase before replication. (A Akhtar, Ed.). PLoS Genet **7**: e1002370.

Li J., Moazed D., Gygi S. P., 2002 Association of the histone methyltransferase Set2 with RNA polymerase II plays a role in transcription elongation. J. Biol. Chem. **277**: 49383–49388.

Lin S., Garcia B. A., 2012 Examining Histone Posttranslational Modification Patterns by High-Resolution Mass Spectrometry. In: *Nucleosomes, Histones & Chromatin Part A*, Methods in Enzymology. Elsevier, pp. 3–28.

Luger K., Richmond T. J., 1998 The histone tails of the nucleosome. Current Opinion in Genetics & Development **8**: 140–146.

MacLean B., Tomazela D. M., Shulman N., Chambers M., Finney G. L., Frewen B., Kern R., Tabb D. L., Liebler D. C., MacCoss M. J., 2010 Skyline: an open source document editor

for creating and analyzing targeted proteomics experiments. Bioinformatics **26**: 966–968.

Margueron R., Justin N., Ohno K., Sharpe M. L., Son J., Drury W. J., Voigt P., Martin S. R., Taylor W. R., De Marco V., Pirrotta V., Reinberg D., Gamblin S. J., 2009 Role of the polycomb protein EED in the propagation of repressive histone marks. Nature **461**: 762–767.

McCloy R. A., Rogers S., Caldon C. E., Lorca T., Castro A., Burgess A., 2014 Partial inhibition of Cdk1 in G 2phase overrides the SAC and decouples mitotic events. Cell Cycle **13**: 1400–1412.

McDaniel S. L., Strahl B. D., 2017 Shaping the cellular landscape with Set2/SETD2 methylation. Cell. Mol. Life Sci. **389**: 1–18.

Morris S. A., Shibata Y., Noma K.-I., Tsukamoto Y., Warren E., Temple B., Grewal S. I. S., Strahl B. D., 2005 Histone H3 K36 methylation is associated with transcription elongation in Schizosaccharomyces pombe. Eukaryotic Cell **4**: 1446–1454.

Muller H. J., 1930 Types of visible variations induced by X-rays inDrosophila. Journ. of Gen. **22**: 299–334.

Olins A. L., Olins D. E., 1974 Spheroid chromatin units (v bodies). Science **183**: 330–332.

Petruk S., Sedkov Y., Johnston D. M., Hodgson J. W., Black K. L., Kovermann S. K., Beck S., Canaani E., Brock H. W., Mazo A., 2012 TrxG and PcG proteins but not methylated histones remain associated with DNA through replication. Cell **150**: 922–933.

Qin S., Min J., 2014 Structure and function of the nucleosome-binding PWWP domain. Trends in Biochemical Sciences **39**: 536–547.

Rao B., Shibata Y., Strahl B. D., Lieb J. D., 2005 Dimethylation of histone H3 at lysine 36 demarcates regulatory and nonregulatory chromatin genome-wide. Mol. Cell. Biol. **25**: 9447–9459.

Rebehmed J., Revy P., Faure G., de Villartay J.-P., Callebaut I., 2014 Expanding the SRI domain family: a common scaffold for binding the phosphorylated C-terminal domain of RNA polymerase II. FEBS Lett. **588**: 4431–4437.

Rechtsteiner A., Ercan S., Takasaki T., Phippen T. M., Egelhofer T. A., Wang W., Kimura H., Lieb J. D., Strome S., 2010 The histone H3K36 methyltransferase MES-4 acts epigenetically to transmit the memory of germline gene expression to progeny. (W Reik, Ed.). PLoS Genet **6**: e1001091.

Reinke V., Gil I. S., Ward S., Kazmer K., 2004 Genome-wide germline-enriched and sex-biased expression profiles in Caenorhabditis elegans. Development **131**: 311–323.

Reinke V., Smith H. E., Nance J., Wang J., Van Doren C., Begley R., Jones S. J., Davis E. B., Scherer S., Ward S., Kim S. K., 2000 A global profile of germline gene expression in C. elegans. Mol. Cell **6**: 605–616.

Samson M., Jow M. M., Wong C. C. L., Fitzpatrick C., Aslanian A., Saucedo I., Estrada R., Ito T., Park S.-K. R., Yates J. R., Chu D. S., 2014 The specification and global

reprogramming of histone epigenetic marks during gamete formation and early embryo development in C. elegans. (R Schneider, Ed.). PLoS Genet **10**: e1004588.

Sankaran S. M., Wilkinson A. W., Elias J. E., Gozani O., 2016 A PWWP Domain of Histone-Lysine N-Methyltransferase NSD2 Binds to Dimethylated Lys-36 of Histone H3 and Regulates NSD2 Function at Chromatin. J. Biol. Chem. **291**: 8465–8474.

Schauer I. E., Wood W. B., 1990 Early C. elegans embryos are transcriptionally active. Development **110**: 1303–1317.

Schmitges F. W., Prusty A. B., Faty M., Stützer A., Lingaraju G. M., Aiwazian J., Sack R., Hess D., Li L., Zhou S., Bunker R. D., Wirth U., Bouwmeester T., Bauer A., Ly-Hartig N., Zhao K., Chan H., Gu J., Gut H., Fischle W., Müller J., Thomä N. H., 2011 Histone Methylation by PRC2 Is Inhibited by Active Chromatin Marks. Mol. Cell **42**: 330–341.

Schneider C. A., Rasband W. S., Eliceiri K. W., 2012 NIH Image to ImageJ: 25 years of image analysis. Nat. Methods **9**: 671–675.

Schuettengruber B., Chourrout D., Vervoort M., Leblanc B., Cavalli G., 2007 Genome Regulation by Polycomb and Trithorax Proteins. Cell **128**: 735–745.

Sidoli S., Bhanu N. V., Karch K. R., Wang X., 2016 Complete workflow for analysis of histone post-translational modifications using bottom-up mass spectrometry: from histone extraction to data analysis. Journal of visualized ….

Sidoli S., Simithy J., Karch K. R., Kulej K., Garcia B. A., 2015 Low Resolution Data-Independent Acquisition in an LTQ-Orbitrap Allows for Simplified and Fully Untargeted Analysis of Histone Modifications. Anal. Chem. **87**: 11448–11454.

Stabell M., Larsson J., Aalen R. B., Lambertsson A., 2007 Drosophila dSet2 functions in H3-K36 methylation and is required for development. Biochem. Biophys. Res. Commun. **359**: 784–789.

Strahl B. D., Allis C. D., 2000 The language of covalent histone modifications. Nature **403**: 41–45.

Strahl B. D., Grant P. A., Briggs S. D., Sun Z.-W., Bone J. R., Caldwell J. A., Mollah S., Cook R. G., Shabanowitz J., Hunt D. F., Allis C. D., 2002 Set2 is a nucleosomal histone H3-selective methyltransferase that mediates transcriptional repression. Mol. Cell. Biol. **22**: 1298–1306.

Strome S., Wood W. B., 1983 Generation of asymmetry and segregation of germ-line granules in early C. elegans embryos. Cell **35**: 15–25.

Tanaka Y., Katagiri Z.-I., Kawahashi K., Kioussis D., Kitajima S., 2007 Trithorax-group protein ASH1 methylates histone H3 lysine 36. Gene **397**: 161–168.

van Kruijsbergen I., Hontelez S., Veenstra G. J. C., 2015 Recruiting polycomb to chromatin. Int. J. Biochem. Cell Biol. **67**: 177–187.

Wagner E. J., Carpenter P. B., 2012 Understanding the language of Lys36 methylation at histone H3. Nature Publishing Group **13**: 115–126.

Wu H., Zeng H., Lam R., Tempel W., Amaya M. F., Xu C., Dombrovski L., Qiu W., Wang Y., Min J., 2011 Structural and histone binding ability characterizations of human PWWP domains. (P Kursula, Ed.). PLoS ONE **6**: e18919.

Xiao T., Hall H., Kizer K. O., Shibata Y., Hall M. C., Borchers C. H., Strahl B. D., 2003 Phosphorylation of RNA polymerase II CTD regulates H3 methylation in yeast. Genes Dev. **17**: 654–663.

Xu C., Bian C., Yang W., Galka M., Ouyang H., Chen C., Qiu W., Liu H., Jones A. E., MacKenzie F., Pan P., Li S. S.-C., Wang H., Min J., 2010 Binding of different histone marks differentially regulates the activity and specificity of polycomb repressive complex 2 (PRC2). Proc. Natl. Acad. Sci. U.S.A. **107**: 19266–19271.

Yuan W., Xu M., Huang C., Liu N., Chen S., Zhu B., 2011 H3K36 methylation antagonizes PRC2-mediated H3K27 methylation. J. Biol. Chem. **286**: 7983–7989.